Quasicrystals. II. Unit-cell configurations

Joshua E. S. Socolar and Paul J. Steinhardt
Department of Physics, University of Pennsylvania, Philadelphia, Pennsylvania 19104-6396
(Received 3 September 1985)

In this (second) paper, quasicrystalline configurations of unit cells are analyzed for the cases of pentagonal and icosahedral orientational symmetry. We illustrate how two ideal quasicrystal structures with the same orientational symmetry and unit cells can be composed from very different local configurations of the cells and emphasize the mathematical and physical significance of subdividing the configurations into local isomorphism (LI) classes. We discuss various methods of constructing quasicrystal unit-cell configurations and techniques for determining the LI classes that the methods generate. Using these techniques, we derive a prescription for constructing the special LI class corresponding to the three-dimensional (3D) icosahedral analogue of the original Penrose tilings (configurations which can be generated by local matching and deflation rules). This prescription is then implemented and the resulting 3D packing is described in detail.

I. INTRODUCTION

An ideal quasicrystal is constructed by the infinite repetition in space of two or more distinct atomic or molecular units, which we refer to as "unit cells," packed in a lattice that has long-range quasiperiodic translational order and long-range orientational order. The orientational symmetry, which can be represented by an arrangement of "star" vectors (see the preceding paper,[1] hereafter denoted as paper I), can be arbitrary in general.

In this paper we wish to focus on a key property of quasicrystal packings of unit cells that has no counterpart in the study of (periodic) crystal packings. For a crystal with fixed orientational symmetry, the ideal structure is defined by a unique packing of a single unit cell. On the other hand, even for a quasicrystal with fixed orientational symmetry and quasiperiodicity, two or more types of unit cells are necessary and there are an infinite number of distinct ideal packings of the unit cells.

We will restrict attention to quasicrystals with two-dimensional (2D) pentagonal or 3D icosahedral orientational symmetry, the examples which are of the greatest physical interest at present. These examples will be used to introduce a mathematical formalism for constructing and classifying the quasicrystal arrangements of unit cells. In particular, it will be shown explicitly how the arrangements fall into different "local isomorphism" (LI) classes as proposed in paper I, where two arrangements are in the same LI class if and only if every finite configuration of cells in each occurs in the other.[2] In Fig. 1, sections of three pentagonal quasicrystal tilings which belong to different LI classes are illustrated. Although they have the same orientational symmetry and unit-cell shapes, the three tilings clearly have very different local (as well as global) configurations of unit cells.

We will discuss methods that have been described in the literature for constructing quasicrystal patterns—the matching and inflation rule approach,[3] the projection methods,[4–7] and the generalized dual method[8] (GDM), or multigrid[9,10] method. The first two approaches will be

shown to generate only a small subset of the possible LI classes. For the case of icosahedral symmetry, the matching and deflation methods and the projection methods produce only a single LI class each. Of the three examples of pentagonal tilings shown in Fig. 1, only the first can be generated by matching and deflation rules or projections.

Distinguishing the LI classes for a given orientational symmetry and quasiperiodicity has mathematical and physical significance. First, because quasicrystal packings belonging to two different LI classes have different local configurations of unit cells, structures obtained by atomic decorations of the unit cells in the packings will generally have two different sets of local atomic environments. In Sec. IV of paper I, other important implications of the existence of LI classes were discussed. We demonstrated that two unit-cell arrangements in different LI classes will, in general, have diffraction peaks at the same wave vectors but will have different peak intensities. Also, atomic arrangements belonging to different LI classes have different free energies. A consequence is that the ground-state configuration of a quasicrystal must be degenerate, corresponding to the same local but different global arrangements of the unit cells, but that *ground-state arrangements must correspond to a single LI class.* Thus, to compute the entropy of a quasicrystal state, which depends upon the number of unit-cell rearrangements with the same energy, one must count only rearrangements in the same LI class.

A case of great mathematical and, potentially, physical interest is the single, special "Penrose local isomorphism" (PLI) class corresponding to arrangements generated by matching and deflation rules [e.g., tiling (a) in Fig. 1]. The original Penrose tiling,[11,12] as described in Sec. II of paper I, is an example of a quasicrystal unit-cell packing that can be forced through local interactions or matching rules that constrain the way two tiles can join edge on edge in the structure. In fact, the mathematical issue that concerned Penrose when he developed his tilings had nothing to do with quasiperiodic packing; he was attempt-

ing to find a set of tile shapes plus matching rules such that the tiles could fill the 2D plane only nonperiodically. Only recently has it been recognized that the pattern is actually quasiperiodic. (The problem of forced nonperiodic tilings has a long and interesting history among mathematicians; we recommend Gardner's article[12] to the reader interested in a more careful definition of the problem and a discussion of its history.) The original Penrose tiling also has the property that the matching rules are equivalent to the constraints placed on adjacent tiles by the requirement of a special self-similarity transformation, also known as a deflation, such that any tiling con-
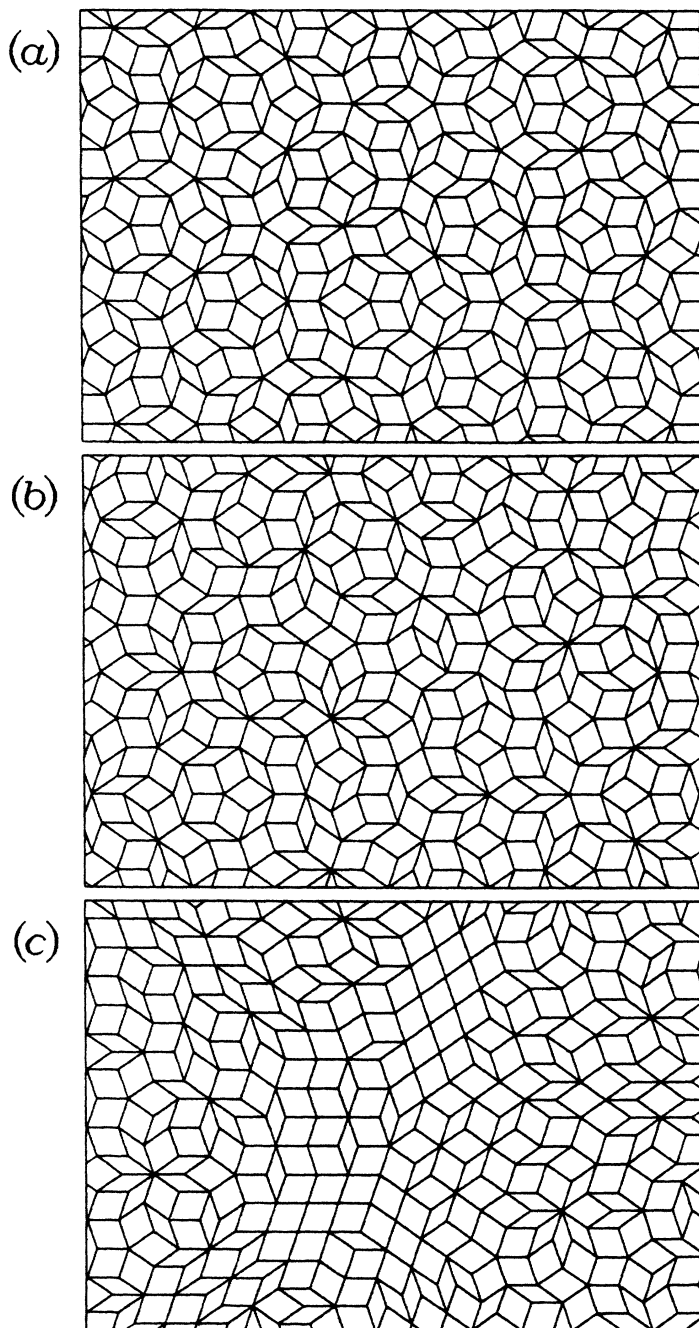

FIG. 1. Characteristic portions of three quasicrystal tilings. Each tiling is the dual to a pentagrid consisting of five grids whose line positions are given by $x_{nN}=N+\alpha_n+(1/\rho)\lfloor N/\sigma+\beta_n\rfloor$. (a) $\rho=\sigma=\tau$. α_n and β_n have values that yield a Penrose tiling. This pattern could also be obtained from a periodic pentagrid or from direct projection from five dimensions. (b) $\rho=\sigma=\tau$. This is an example of the dual of a general Fibonnacci pentagrid. (The values of α_n and β_n were chosen at random.) Note that this pattern contains adjacent tiles of the same type and orientation and therefore could not be obtained as the dual to a periodic pentagrid (see Secs. IV B and IV C). (c) $\rho=2^{-5/2}$, $\sigma=3^{3/2}$. This is the dual of a non-Fibonnacci quasiperiodic pentagrid.

sistent with the matching rules can also be obtained by a repeated deflation of an initially small cluster of tiles.

One of the goals of this paper is to present the detailed construction of the 3D icosahedral analogue to the Penrose tilings—the 3D icosahedral PLI class. The 3D analogue is significantly more subtle than the 2D case, for reasons that will be discussed later. The construction method has been applied to find analogues with other symmetries, including the case of 2D octagonal symmetry,[13] but we do not know how to extend the approach to arbitrary symmetry.

The potential physical interest in the special PLI class of pentagonal and icosahedral tilings is that the matching rules may have physical manifestations in some atomic structure through the local interactions of atoms or atomic clusters. These interactions could insure that the quasicrystal state is energetically preferred and that the ground state corresponds to the PLI class. It may even be possible to "design" covalently bonded atomic systems or complex molecules to enforce such matching rules. We should emphasize that we have no reason to suggest that the icosahedral phase of aluminum and manganese (I-Al-Mn) (Ref. 14) corresponds to the icosahedral PLI class. However, even if I-Al-Mn does not belong to the PLI class, the ground-state configuration of a quasicrystal does correspond to some single LI class. It is at least worthwhile to study the PLI class as a particular example of an LI class; its special properties make it easy to analyze.

In paper I, we introduced the general notion of quasicrystals, discussed the classification of quasicrystals according to orientational symmetry and quasiperiodicity, proved various properties about the diffraction patterns of quasicrystals, and discussed some atomic modeling of 2D pentagonal quasicrystals.

The organization of paper II is as follows. In Sec. II we establish some terminology and briefly review various methods for constructing quasicrystal packings of unit cells. In Sec. III we discuss 1D quasicrystals. We apply the numerous methods that have been devised for constructing quasicrystals—deflation rules, projections, and GDM—to construct the 1D analogue. We show that for one dimension the methods are essentially equivalent and we describe some advantages of each. In Sec. IV we apply the various construction methods to the case of 2D pentagonal quasicrystals. We demonstrate that the GDM generates a much larger set of LI classes than the other methods and show how to fix the free parameters in the GDM construction so as to obtain the PLI class. In Sec. V we extend the analysis to the case of 3D icosahedral quasicrystals. We show that in this case the projection method (from six dimensions) produces only a single LI class of tilings. We then present the detailed construction of the PLI class using the GDM. Our concluding remarks are given in Sec. VI.

II. QUASICRYSTAL UNIT-CELL PACKINGS

A (periodic) crystal or quasicrystal is constructed from the repetition in space of structural motifs called unit cells. In either case, even if the orientational symmetry is fixed, the identification of the number of unit cells or the unit-cell shapes is not unique. For example, for a crystal with square symmetry one possible set of unit cells consists of one element: the square; however, another set consists of two shapes: an octagon, to replace each of the squares above, and a small square, which fills the gaps between the octagons. The first set leads to a packing that corresponds to the square Bravais lattice and it is clearly the simplest. For the quasicrystal, sets of unit cells composed of 2D rhombuses or 3D rhombohedra appear to be the most useful, although Penrose has provided at least four different sets of unit-cell shapes (ranging from two to six elements) that can all form pentagonal quasicrystal packings.[12,15]

In this paper we restrict attention to quasicrystal packings of rhombic and rhombohedral unit cells. In order to discuss methods of constructing and comparing quasicrystal packings of unit cells, it is useful to establish some basic terminology and concepts. Many of the terms have been introduced by other authors, particularly by de Bruijn.[9] The reader should be aware, however, that some definitions differ slightly from other usages in order to facilitate our discussion of a wide class of quasicrystal packings (and symmetries).

A. Definitions

The following terms will be defined first for the case of 2D quasicrystals. The extension of the definitions to the three dimensions is then given in parentheses where necessary. Extension to yet higher dimensions is straightforward.

(1) A 2D *grid* is an infinite set of nonintersecting infinite (open) coplanar curves. The curves in a grid can be labeled by integers corresponding to their ordinal position in the grid. (A 3D *grid* is an infinite set of nonintersecting, simply connected, infinite (unbounded) surfaces in a 3D space. The surfaces in a grid can be labeled by integers corresponding to their ordinal position in the grid.) Assigned to a grid is a "star" vector which plays an important role in the dual construction (see Sec. II B).

(2) A 2D *N-grid* is a set of N grids with the property that each curve in the ith grid intersects each curve in the jth grid at exactly one point for all $i \neq j$. If more than two curves meet at a point in the N-grid, the N-grid is called *singular*.[9] (A 3D *N-grid* is a set of N grids with the property that any triplet of surfaces belonging to the ith, jth, and kth grids, respectively, where $i \neq j \neq k$, intersect at exactly one point. Any pair of surfaces belonging to the ith and jth grids, respectively, where $i \neq j$, intersect along a single infinite (open) curve. If more than three surfaces meet at a point, the N-grid is said to be *singular*.)

(3) A *quasilattice* (QL) is a set of points with the following properties.

QL1: The points lie at the intersections of an N-grid.

QL2: The number of different cell shapes obtained via the Voronoi construction[16] about each point is finite.

QL3: The set of points exhibits quasiperiodic translational order.

In the same sense that the term lattice can refer to a set of

points or to the lines (or planes) at whose intersection they lie, the term quasilattice will refer to a set of points or to the N-grid (in QL1). Note that QL2 implies the existence of a minimum distance between neighboring sites and a maximum distance between nearest neighbors. The packing of Voronoi cells itself satisfies the definition of quasicrystal given in paper I. For many applications, however, it is more useful to consider the packing of rhombuses or rhombohedra obtained as a dual to the N-grid[9,4,8] since it contains fewer unit-cell shapes. The term quasiperiodic translational order in QL3 means, for example, that the function obtained by associating a delta function with each lattice site has a Fourier transform consisting of Bragg peaks whose positions are generated by linear combinations of $d + 1$ or more independent wave vectors, where d is the number of dimensions.

(4) A *linear grid* is an infinite set of parallel lines, or a grid composed of straight lines. A vector $\mathbf{e}$ normal to these lines defines the *direction of the grid*. (A *planar grid* is an infinite set of parallel planes or a grid composed flat planes. A vector $\mathbf{e}$ normal to the planes defines the *direction of the grid*.) Each line or plane in the grid is defined by the equation

$$\mathbf{x} \cdot \mathbf{e} = x_N, \quad N \in \mathbf{Z} , \tag{1}$$

where x_N is a monotonically increasing sequence in N.

(5) A *periodic grid* is a linear (or planar) grid in which the sequence x_N is periodic. In this paper we will use the term to refer to the special case of grids with *equal* spacing between grid lines given by some constant, T. In this case, the periodic grid is totally specified by T and a single real number γ, corresponding to the phase of the grid with respect to the origin. For a periodic grid

$$x_N = T(N + \gamma) . \tag{2}$$

(6) A *quasiperiodic grid* is a linear or planar grid in which the sequence x_N is quasiperiodic. In this paper we will consider as an example quasiperiodic sequences of the form:

$$x_N = T \left[N + \alpha + \frac{1}{\rho} \left\lfloor \frac{N}{\sigma} + \beta \right\rfloor \right] , \tag{3}$$

where α, β, and $\rho \in \mathbf{R}$, σ is irrational, and "$\lfloor \ \rfloor$" denotes the greatest integer function ("floor function"). Without loss of generality, we take $\sigma, \rho > 0$. The expression defines a quasiperiodic sequence of long and short spacings of length $T(1 + 1/\rho)$ and T, respectively, where σ determines the relative frequency of the two different spacings in the sequence and ρ determines the ratio of the two spacing lengths that occur between grid lines. The choice $\rho = \sigma = \tau$, where $\tau [\equiv (1 + \sqrt{5})/2]$ is the golden mean, corresponds to a *Fibonacci* sequence. (See paper I for a description of the properties of a Fibonacci sequence.) The effect of a change in α is simply to translate the entire grid in the direction of $\mathbf{e}$, whereas a change in β can alter the sequence of long and short spacings.

(7) A *linear N-grid* is an N-grid composed of linear grids. (A *planar N-grid* is an N-grid composed of planar grids.) Although this paper deals almost exclusively with

linear 5-grids with pentagonal symmetry and planar 6-grids with icosahedral symmetry, it should be noted that arbitrary symmetries are possible.[8]

(8) A *periodic pentagrid* is a 2D (linear) periodic 5-grid composed of five sets of grids each oriented normal to one of the vectors

$$\mathbf{e}_n = (\cos(2\pi n/5), \sin(2\pi n/5)), \quad n = 0, 1, \ldots, 4 .$$

If the periodic spacing between lines is taken to be unity, the grid in the nth direction is completely specified by γ_n [see Eq. (2)] and we can use the notation $\{\gamma_n\}$ to represent a periodic pentagrid. Note that de Bruijn[9] has used the term "pentagrid" to refer to a subset of 5-grids which are, according to our definition, periodic pentagrids.

(9) A *periodic hexagrid* is a 3D (planar) periodic 6-grid for which each grid is oriented normal to one of the six independent fivefold symmetry axes of an icosahedron, and the periodic hexagrid can be specified by the $\{\gamma_n\}$ (where n runs from 0 to 5) associated with the six constituent grids. Note that the hexagrids obtained by Kramer and Neri[4] via (grid) projection methods are periodic hexagrids.

(10) A *quasiperiodic pentagrid* is a 5-grid composed of *quasiperiodic* grids with directions

$$\mathbf{e}_n = (\cos(2\pi n/5), \sin(2\pi n/5)), \quad n = 0, \ldots, 4 .$$

To completely specify the quasiperiodic pentagrid we must specify ρ_n, σ_n, α_n, and β_n for each n [see Eq. (3)]. The generalization to a *quasiperiodic hexagrid* is straightforward.

(11) A *Fibonacci pentagrid* is a quasiperiodic pentagrid based on sequences of the form in Eq. (3) with $\rho_n = \sigma_n = \tau$, for all n (Fibonacci sequences). The only degrees of freedom left in this case are the α_n and β_n, so we will use the notation $\{\alpha_n, \beta_n\}$ to represent the Fibonacci pentagrid. (The generalization to *Fibonacci hexagrids* is straightforward.) It can be shown that the intersections of a Fibonacci pentagrid form a quasilattice.

(12) The *skeleton* of a 2D quasicrystal packing of rhombic unit cells is a quasilattice decoration of the packing that can be constructed as follows: In each rhombus, construct the two line segments joining the midpoints of opposite edges and with each of these segments associate a vector that points in the direction of the edges (the ambiguity of the sign of the vector must be resolved in the same way for every segment that connects edges of the same orientation). The line segments join to form sets of continuous jagged curves that form a quasilattice. The quasilattice is referred to as the skeleton of the tiling. (In 3D, the skeleton is formed by planar sections which bisect opposite faces of the rhombohedra in the quasicrystal packing. The planar sections join to form connected jagged surfaces that form a quasilattice decoration of the packing.)

(13) A *grid-space* is the space in which an N-grid lies, including the case of N-grids corresponding to quasilattices and skeletons. A dual transformation maps a grid space into a *cell space* such that open regions in grid space are mapped into points in cell space and points in grid space are mapped into open regions in cell space.

B. Methods of constructing quasicrystal packings

Several methods have been developed for constructing quasicrystal packings of unit cells. It is useful to carefully distinguish the techniques in order to determine their relative advantages.

The "matching and deflation rule" approach[3] is the one which most closely resembles the approach used to construct the original Penrose tiling. A deflation rule is a self-similarity transformation in which each unit cell can be subdivided into pieces that can rejoin to form a new quasicrystal packing with all unit cells scaled down by some constant factor. Thus, a unit-cell packing can be obtained by successive application of the deflation rule beginning from a small cluster of unit cells. In some cases, there exists a set of matching rules in one-to-one correspondence with the deflation rules; that is, the matching rules constrain how the unit cells can pack together edge on edge (or face on face) such that the unit cells can fill space only in quasicrystal arrangements obtainable by repeated deflation. The matching and deflation rule approach produces only a single LI class that we term the Penrose local isomorphism (PLI) class, since the original Penrose tilings are examples of the PLI class for the case of pentagonal symmetry. We have been able to fully extend this approach for the case of 3D icosahedral symmetry.

The "grid projection" approach, due to de Bruijn[9] and Kramer and Neri,[4] is a method of obtaining a linear or planar periodic N-grid as a projection from a higher-dimensional periodic lattice. The vertices of the unit-cell packing are then obtained by a "dual" transformation, the same as we will describe in the discussion of the generalized dual method (GDM). It should be noted that it is straightforward to construct a periodic N-grid in a grid space without any reference to higher dimensions. The grid projection approach can be extended to arbitrary symmetry, but has been discussed only for periodic pentagrids.[17,10]

The "direction projection approach," developed by Elser,[6] Kalugin et al.,[5] and Duneau and Katz,[7] obtains the vertices of a quasicrystal packing of unit cells directly (without taking a dual) by projecting points from a higher-dimensional periodic lattice. Depending upon the orientational symmetry, a lower-dimensional projection plane (corresponding to the real space) is chosen and all points within a special strip about the plane are projected orthogonally onto the plane. The strip must be specially chosen so that the projected points produce a complete set of vertices for a quasicrystal unit-cell packing. It has been suggested that the method can be extended to produce packings with arbitrary symmetry.[7,10] This method is powerful because it leads to an elegant and straightforward method for computing the diffraction pattern of the packing of unit cells. On the other hand, the method leads to only a restricted set of LI classes for a given symmetry. For example, icosahedral quasicrystal packings obtained via direct projections from six dimensions to three dimensions correspond to only a *single* LI class.

The "generalized dual method,"[8] or multigrid method[9,10] is a method for constructing a much wider class of quasicrystal packings (different LI classes) than

the other methods for a given orientational symmetry. In addition, the method can be used to construct quasicrystal packings with *arbitrary* symmetry. The one disadvantage is that there is no direct analytic method known for finding the diffraction pattern of a general GDM quasicrystal packing. Although the details of the construction method are given in Ref. 8, we will briefly recount the method. Given an arbitrary (not necessarily periodic or linear) N-grid in a grid space, a unique star vector, e_i, is associated with each of the N grids.[18] Each open region (a region bounded by grid lines through which no other grid lines pass) in the N-grid is characterized by N integers, k_i: for each $i \leq N$, the open region lies between the grid curves (or surfaces) which are associated with the e_i direction and which are labeled k_i and k_{i+1}, respectively. The "dual" transformation associates with each open region in the grid space the point

$$t = \sum_{i=1}^{N} k_i e_i .$$

If each of the grids is quasiperiodic, the set of vertices, t, is guaranteed to form a full quasicrystal packing of unit cells with orientational symmetry corresponding to the star vectors, e_i.

III. ONE-DIMENSIONAL QUASICRYSTALS

Even though there is no analogue of orientational order in one dimension, 1D quasicrystals are useful for illustrating several important properties of quasicrystal structures. Most of the features of 1D quasicrystals we will discuss apply directly to 2D and 3D quasicrystals with crystallographic orientational symmetry (incommensurate crystals) as well, since these structures are, in some sense, direct products of uncoupled 1D quasicrystals. For quasicrystals with noncrystallographic (e.g., pentagonal or icosahedral) orientational symmetry, the degrees of freedom *are* coupled, and there are new features and physical properties.

For the purposes of this discussion, we will consider ideal 1D quasicrystals with atomic positions, x_N, given by

$$x_N = N + \alpha + \frac{1}{\rho} \left\lfloor \frac{N}{\sigma} + \beta \right\rfloor , \qquad (4)$$

where $\lfloor x \rfloor$ is the greatest integer less than x, $\sigma > 1$ is an irrational number,[19] and $\rho > 0$, α, and β are arbitrary real numbers. The 1D analogue of a "packing of unit cells" is a "sequence of intervals." Equation (4) describes a sequence of atomic sites such that the interval between sites, $\Delta x \equiv x_N - x_{N-1}$, has the property:

$$\Delta x = \begin{cases} 1, & \text{if } \left\lfloor \dfrac{N}{\sigma} + \beta \right\rfloor - \left\lfloor \dfrac{N-1}{\sigma} + \beta \right\rfloor = 0 , \\[4mm] 1 + \dfrac{1}{\rho}, & \text{if } \left\lfloor \dfrac{N}{\sigma} + \beta \right\rfloor - \left\lfloor \dfrac{N-1}{\sigma} + \beta \right\rfloor = 1 . \end{cases} \qquad (5)$$

That is, there are only two possible intervals between sites, $L = 1 + 1/\rho$ and $S = 1$, which appear in a quasiperiodic sequence where the ratio of the number of L's to the

number of S's equals $1/(\sigma-1)$. Thus, the parameters ρ and σ determine the relative intervals and frequencies in the sequence. A case of special interest is $\rho=\sigma=\tau$, corresponding to the *Fibonacci* sequence (see paper I), which also plays a central role in the construction of pentagonal and icosahedral quasicrystal packings of unit cells.

A. 1D quasicrystals and local isomorphism

There are an infinite number of quasiperiodic arrangements of intervals with the same two lengths and frequencies. These different arrangements correspond to different choices of α and β for fixed ρ and σ. In higher dimensions, we will want to discuss the possible arrangements of unit cells (the analogues of intervals in one dimension) and classify arrangements according to the "local ismorphism" (LI) class. In one dimension the precise definition of local isomorphism is as follows.

Definition: Two 1D quasicrystals are *locally isomorphic* (or, equivalently, in the same LI class) if and only if given any point P in either structure and any finite distance d, there exists a translation of the other structure such that the (atomic) positions x_N coincide exactly from P out to at least distance d.

Two 1D quasicrystal sequences that are related by a pure translation are obviously in the same LI class according to this definition. Two 1D quasicrystals are not in the same LI class if there exists even a single finite subsequence of intervals in one that does not occur in the other.

For fixed ρ and σ, we can show that the 1D quasicrystals described by Eq. (4) are in the *same* LI class for all (α,β). (The 1D case is trivial in this sense, but the analogue construction in higher dimensions results in many inequivalent LI classes, as we shall show in later sections.) First, shifts in α correspond to pure translations of the quasicrystals and so two quasicrystals (α,β) and (α',β) are obviously in the same LI class according to the definition above.

The fact that (α,β) and (α,β') are in the same LI class is less obvious. First, it is useful to note that transformations of the form:

$$\alpha\rightarrow\alpha+p+\frac{q}{\rho}\ ,$$
$$\beta\rightarrow\beta-q+\frac{p}{\sigma}\ ,$$

(6)

where p and q are integers, leave a 1D quasicrystal completely unchanged—the sites and sequence of intervals are the same, although the integer label for a given site may change. We shall refer to this special class of discrete transformations as an *umklapp*. In some sense, it plays the same role for quasicrystals as the translation by a single lattice spacing does for periodic crystals. If quasicrystals (α,β) and (α',β') are related by an umklapp, they are identical. In general, we will refer to two quasicrystals (α,β) and (α',β') related by a translation plus an umklapp as being *umklapp congruent*. Two sequences that are umklapp congruent are obviously in the same LI class. Note also that if quasicrystals A and B are umklapp congruent

to C, then they are umklapp congruent to one another.

Theorem 3.1. (α,β) and (α',β') are in the same LI class.

Proof: Choose any site P in (α,β). The sequence (α,β) can be translated to a sequence (α'',β) where the point P corresponds to x_0. Now, first suppose that $\beta'-\beta$ is of the form $-q+p/\sigma$ for some pair of integers p and q. Then the sequence (α',β') can be translated

$$\alpha'\rightarrow\alpha''+p+\frac{q}{\rho}$$

and the translated sequence $(\alpha''+p+q/\rho, \beta-q+p/\sigma)$ is clearly an umklapp of (α'',β), which is a translate of (α,β). Thus the two sequences are umklapp congruent and are in the same LI class.

Next, suppose $\beta'-\beta$ cannot be expressed in the form $-q+p/\sigma$. Nevertheless, because σ is irrational, $\beta'-\beta$ can be approximated arbitrarily well by expressions of this form; that is, for every δ there exist integers p and q such that

$$\beta'-\beta=-q+\frac{p}{\sigma}+\epsilon\ ,$$

where $\epsilon<\delta$. Since we can translate $\alpha'\rightarrow\alpha''+p+q/\rho$, (α',β') is umklapp congruent to $(\alpha'', \beta+\epsilon)$ for arbitrarily small ϵ. From Eq. (4) we see that (α'',β) and $(\alpha'',\beta+\epsilon)$ are identical for sites ranging from $N=0$ (corresponding to site P) up to $N=\hat{N}$, where $\hat{N}$ is the smallest integer such that

$$\left\lfloor\frac{\hat{N}}{\sigma}+\beta\right\rfloor\neq\left\lfloor\frac{\hat{N}}{\sigma}+\beta+\epsilon\right\rfloor\ .$$

As ϵ approaches zero, this occurs only for increasing values of $\hat{N}$ approaching infinity. Note that this same argument would work if we began with some point P in (α',β') and umklapped (α,β). Thus, by the definition above, the two sequences are in the same LI class.

Note that in the last case, the two sequences are not umklapp congruent. Although they are identical up to any finite distance, there is no finite translation of one such that the two sequences coincide out to infinite distances.

B. Methods of constructing 1D quasicrystals

Although the 1D case is significantly more trivial than the higher-dimensional analogues, it is instructive to compare the different methods of constructing unit-cell packings for 1D quasicrystals.

1. Deflation rule approach

There is probably not any (local) matching rule for the intervals that will force a quasicrystal packing.[20] We can still, however, discuss deflation rules in one dimension—self-similarity transformations that divide each interval in a 1D quasicrystal into subintervals that form a new quasicrystal sequence of intervals. The deflation rules, as discussed in Ref. 3, are relevant to sequences defined by *algebraic numbers,*[21] numbers which are roots of polynomial equations with integer coefficients. (These are also the

cases relevant to quasicrystals with orientational symmetry corresponding to some polygon in two dimensions or polyhedron in three dimensions.) The *degree* of an algebraic number is the degree of the lowest-order polynomial equation satisfied by that number.

We shall first consider the case of 1D quasicrystals corresponding to Eq. (4) with the Fibonacci sequence,

$$\rho = \sigma = \tau \equiv \frac{1+\sqrt{5}}{2} \ .$$

All neighboring atoms are separated by either L or S where $L = \tau$ and $S = 1$. The sequence of L and S intervals has the property that it is invariant under a "substitution rule" or "deflation rule" of the form:

$$\begin{bmatrix} L \\ S \end{bmatrix} \rightarrow \begin{bmatrix} 1 & 1 \\ 1 & 0 \end{bmatrix} \begin{bmatrix} L \\ S \end{bmatrix} \ . \tag{7}$$

The deflation rule means that each L in the sequence is replaced by the pair of intervals LS and each S in the sequence is replaced by an L. When this procedure is carried out another Fibonacci sequence is obtained [though usually with a different value of α and β in Eq. (4)]. An equivalent deflation rule (up to a translation) is

$$L \rightarrow \frac{L}{2} S \frac{L}{2}, \ \ S \rightarrow \frac{L}{2} \frac{L}{2} \ , \tag{8}$$

which is depicted in Fig. 2. We have chosen this last definition for the analysis in this paper.

Now let us consider how deflation acts on the parameters of the 1D quasicrystal defined by the Fibonacci sequence,

$$x_N = N + \alpha + \frac{1}{\tau} \left\lfloor \frac{N}{\tau} + \beta \right\rfloor \ . \tag{9}$$

A minor caveat to our treatment here is the special care must be taken if β is a number of the form $k + l/\tau$ where k and l are integers (i.e., β is in the ideal of τ), in which case $\beta + N/\tau$ is equal to an integer for some N. Throughout this paper we assume that β is not of this form (unless otherwise stated). This case requires special treatment at all stages and adds nothing of interest to our results.

A deflation of a 1D quasicrystal sequence according to Eq. (4) and Fig. 2 is given by a transformation of the α and β:
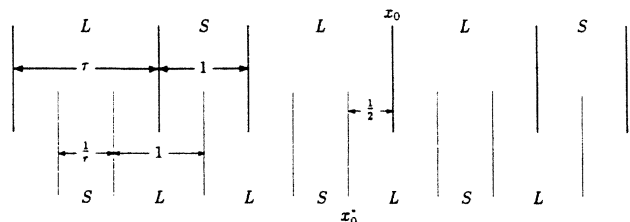

FIG. 2. Unscaled deflation of a Fibonnacci grid. The original grid is shown on top. The deflation is performed according to Eq. (8). The $N = 0$ lines of the original and unscaled deflated grids are marked by x_0 and x_0^*, respectively.

$$\alpha^* = \tau \left[\alpha + \frac{\lfloor \beta \rfloor}{\tau} - \frac{1}{2} \right] - \frac{\lfloor \beta^* \rfloor}{\tau} \ , \tag{10}$$

$$\beta^* = \frac{1}{\tau} (\lfloor \beta \rfloor - \beta) \ . \tag{11}$$

(The asterisk indicates a parameter of a deflated sequence.) Stolarsky,[22] de Bruijn,[9] and others have derived Eq. (11) by considering the action of a deflation on the *order* of long and short intervals with a specific convention for determining the zeroth interval. We have derived Eq. (10) which insures that the left-hand end point of the zeroth interval of the deflated sequence corresponds to x_0^* (see Fig. 2). Note that the intervals in the deflated sequence have been scaled by τ so that the lengths in it are the same as in the original. This formula becomes a bit more transparent if one notes that the quantity $\alpha + \tau^{-1} \lfloor \beta \rfloor$ is just x_0, so that Eq. (10) can be rewritten as

$$x_0^* = \tau (x_0 - \tfrac{1}{2}) \ . \tag{12}$$

Figure 2 illustrates this relation. *These transformation rules shall play a very important role in our discussion of pentagonal and icosahedral quasicrystals.*

In Ref. 3, the most straightforward extension of deflation rules to other sets of algebraic numbers was discussed. One begins with k lengths (L_i), at least some of which must be incommensurate. Then there is a substitution rule:

$$(L_i) \rightarrow M_{ij} (L_j) \ , \tag{13}$$

where the matrix M_{ij} is a $k \times k$ nonsingular matrix with non-negative integer coefficients. It must also have irrational eigenvalues which, because M_{ij} has integer coefficients, must satisfy a polynomial equation of kth degree (i.e., be algebraic numbers). If the matrix is irreducible in the sense that it cannot be block diagonalized, we say the substitution rule describes a k-component quasicrystal.

There remain many interesting open issues concerning deflation rules. First, we do not know how to obtain a closed-form expression, such as Eq. (4), appropriate to a general deflation rule. Simple expressions utilizing the greatest integer function, such as Eq. (4), are only relevant (so far as we know) to cases where ratios of length scales and frequencies are algebraic numbers of degree two (quadratic irrationals). This is related to the fact that the greatest integer function is useful in determining rational approximants to quadratic irrationals.[21] Second, we do not know how to compute the diffraction pattern associated with a quasicrystal sequence generated by a general deflation rule. [It is straightforward to compute the diffraction pattern of any of the sequences generated in Eq. (4) using the methods described in paper I. Up to an overall scale factor, the location of the peaks is identical for fixed σ, independent of ρ]. In fact, if the substitution matrix for a deflation rule has more than two eigenvalues of modulus greater than unity, we do not know if the Fourier transform converges to true Dirac δ functions.[23] Third, one can consider the possibility of deflation rules involving more than just a single substitution rule. For example, one can consider the possibility of using a sequence of substitution rules, or different substitutions for different

elements of the same length. This can lead to a situation where the deflation of an interval of given length depends upon its place in the sequence of intervals. (Pleasants terms these "bounded context inflations."[24]) The 1D quasicrystals obtained by direct projection from a 2D periodic lattice to a 1D quasicrystal sequence where ρ and σ are algebraic numbers of degree three or higher appear to correspond to deflation rules of this more complicated type.[24]

Because we find the matching and deflation approach the most difficult to study analytically and to generalize, we generally prefer the GDM approach. Nevertheless, the deflation approach is the most straightforward way of obtaining a 1D quasicrystal with simple self-similarity transformations (which is difficult and sometimes impossible to obtain by the other methods[24]). *Furthermore, the notion of deflation rules are critical for identifying the special Penrose local isomorphism class in 2D and 3D, as we shall see.*

2. Direct projection approach

Although the direct projection approach has been discussed for 1D quasicrystals elsewhere,[6,9,24,25] we wish to present it (in a slightly more general context) in order to relate it to other approaches.

In the direct projection approach, the positions of sites in the 1D quasicrystal sequence, x_N, are obtained by projection from a 2D periodic lattice onto a line. Only a subset of points in the periodic lattice lying within a specially chosen strip about the projection line are projected. Thus, *both the projection line and the strip are critical components in the direct projection approach.*

To obtain 1D quasicrystals corresponding to the sequences described in Eq. (4), consider a 2D periodic lattice with rectangular unit cells of dimensions $\hat{a} \times \hat{b}$ whose edges are aligned with the x and y axes, respectively. Next, construct a projection line oriented at angle θ with respect to the x axis. (See Fig. 3.) For only a small subset of unit cells does the projection line pass through the right-hand vertical edge of the unit cell. If the lower right-hand vertex, say, of each such unit cell is projected orthogonally onto the line, it produces a sequence of points described by Eq. (4).

To establish this result, it is useful to distinguish three sets of points in Fig. 3. First, marked by open squares is a set of points that we will call *grid points* corresponding to the intersections of the projection line with vertical lines of the lattice. The intersection with the mth vertical line has coordinates $(m\hat{a}, m\hat{a}\tan\theta + y_0)$, where y_0 is the y intercept of the projection line. Next, marked by open circles is the set of points corresponding to the lower right-hand corner of each unit cell for which the projection line passes through the right-hand vertical edge. Their coordinates are

$$\left[m\hat{a}, \left| m\frac{\hat{a}}{\hat{b}}\tan\theta + \frac{y_0}{\hat{b}} \right| \hat{b} \right] .$$

Third, there are the projections of these points onto the projection line, indicated by the solid circles. Their coor-

dinates along the projection line (up to an overall translation) are

$$x_N = N\hat{a}\cos\theta + \hat{b}\sin\theta \left| N\frac{\hat{a}}{\hat{b}}\tan\theta + \frac{y_0}{\hat{b}} \right| .$$

If we choose $\hat{a}\cos\theta = 1$, $\hat{b}\sin\theta = 1/\rho$, and

$$\frac{\sin\theta}{\hat{b}\cos^2\theta} = \frac{1}{\sigma} ,$$

we obtain

$$x_N = N + \frac{1}{\rho}\left| \frac{N}{\sigma} + \frac{y_0}{\hat{b}} \right| \tag{14}$$

which is the same as Eq. (4) with $\alpha = 0$ and $\beta = y_0/\hat{b}$.

From this analysis, it is clear that shifts in the angle θ, or the unit-cell dimensions, $\hat{a}$ and $\hat{b}$, change the values of ρ and/or σ. Changes in the y intercept, y_0, only change β; that is, according to Sec. III A, they correspond to shifts from one element of the LI class to another. A shift in the 2D periodic lattice by $p\hat{a}$ in the x direction and $q\hat{b}$ in the y direction for integers p and q leave the 2D lattice invariant and their projections correspond to umklapp transformations of the 1D quasicrystal. Instead of specifying the projected points as corresponding to the lower right-hand corner of certain rectangles, we could have defined a strip extending from the projection line to a line parallel to it but with y intercept, $y_0' = y_0 - \hat{b}$ (see Fig. 3); then the lower right-hand corner points that are projected correspond to exactly that set of points in the
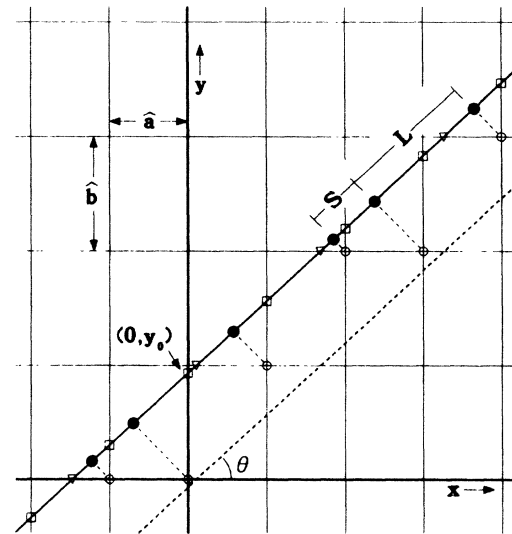

FIG. 3. Illustration of techniques for obtaining 1D quasicrystal sequences by projection from a 2D lattice. The solid circles are the points of the quasicrystal sequence. They lie on the projection line. The open squares and triangles are the grid points for the grid projection approach (and the GDM). The open circles are the points which are projected orthogonally in the direct projection method. The projection strip, which determines the lattice points that get projected, is the open strip between the projection line and the parallel dashed line in the figure.

2D periodic lattice that lie in the strip. For the Fibonacci sequence, the deflation rules discussed in Sec. III B 1 correspond to a transformation of the projection strip to a wider strip.[24,6] For this example, where $\rho = \sigma = \tau$, the 2D periodic lattice has a square unit cell and the projection angle with respect to the x axis satisfies $\tan\theta = 1/\tau$. The projection strip described above has width $\hat{b}\cos\theta = 1$ (in the units defined above) and lies just below the projection line; this includes the lower right-hand vertices that were projected. A single deflation corresponds to adding a strip section of width $\hat{a}\sin\theta = 1/\tau$ above the projection line. Pleasants[24] has discussed the generalization of this deflation to other projection angles in which $\tan\theta$ corresponds to an algebraic number. For most cases, the deflation is of the more complicated sort described in Sec. III B 1 in which the deflation of an interval of given length depends upon the neighborhood of intervals that surround it (a so-called "bounded context" inflation). Nevertheless, there does exist a self-similarity transformation of some sort when irrational ratios correspond to algebraic numbers.

In one dimension the quasicrystal sequence is both a quasilattice and the 1D analogue of a unit-cell packing. In higher dimensions though, the quasilattice and the unit-cell packing are distinct, although one can be considered the decoration of the other. The diffraction pattern of the quasilattice is simple to compute from the diffraction pattern of the 1D sequence. The diffraction pattern for the 1D sequence described in Eq. (4) can be compute via a straightforward generalization of the method described in Sec. III A of paper I. The chief advantage of the direct projection method is that it leads to a simple and elegant method of computing the diffraction pattern of the unit-cell packing (rather than the quasilattice) in higher dimensions. Briefly, the vertices of the unit-cell packing in two or three dimensions are projected vertices of a higher-dimensional periodic lattice that lie in a projection strip about a projection plane. The diffraction pattern of the packing is obtained by convoluting the Fourier transform of the higher-dimensional lattice with the Fourier transform of the characteristic function of the strip (a function whose value is unity inside the strip and zero outside the strip) and then projecting to two or three dimensions. This construction makes it more obvious why the diffraction pattern consists of a dense set of Bragg peaks; the diffraction pattern of the higher-dimensional lattice consists of a periodic reciprocal lattice of Bragg peaks which project into a dense set of Bragg peaks in the lower dimension. However, the detailed computational method is no simpler than the method required to compute the diffraction pattern of the quasilattice.

3. Grid projection and generalized dual method

Although the grid projection and generalized dual method (GDM) are very useful methods for obtaining unit-cell packings in higher dimensions, in one dimension they appear unnecessarily complex. Nevertheless, to complete the discussion, we will discuss the 1D construction.

For both the grid projection method and the GDM, the first step is to create an N-grid. The dual to the N-grid

yields the 1D quasicrystal sequence in either method. A 1D grid consists of a sequence of points which are labeled by integers according to their ordinal position in the sequence. A 1D N-grid, then, consists of N grids along the same line. (Note that, whereas grid curves in two dimensions or grid surfaces in three dimensions belonging to different grids must intersect in an N-grid, there is no analogue intersection condition in one dimension). Assigned to each grid is an interval length L_i, which plays an important role in the dual construction. To obtain the 1D quasicrystal sequence described by Eq. (4), a 1D 2-grid is required.

In the grid projection method, the 2-grid is obtained as a projection from higher dimensions. First, some higher-dimensional periodic lattice and projection plane is chosen, say the 2D periodic lattice shown in Fig. 3. Next, the horizontal and vertical lines in the 2D periodic lattice are "projected" along the x and y axes, respectively, onto points along the projection line to form two "grids." The two sets of grid points correspond to the intersection of the lattice lines with the projection line, as shown by the open squares and open triangles in Fig. 3. The 2-grid is thus defined by dividing the grid points into two overlapping grids, one set consisting of intersections with vertical lattice lines (grid 1) and the other consisting of intersections with horizontal lattice lines (grid 2). Each set of grid points is indexed by an integer corresponding to its ordinal position in the grid. Note that it is straightforward to proceed with the construction of the 2-grid directly in the 1D space without reference to projections, as is done in the GDM: two overlapping periodic sequences of points whose periods are in the ratio σ:1 are constructed on a 1D lattice. Not only is the GDM construction of the 2-grid straightforward, but it can easily be generalized to quasiperiodic (rather than periodic) 2-grids.

Once the 2-grid is obtained by either method (periodic or quasiperiodic), an interval length (the analogue of a star vector in two or three dimensions) is assigned to each grid: for the example in Fig. 3, interval length $L = 1 + 1/\rho$ is assigned to grid 1 and interval length $S = 1$ is assigned to grid 2.

The dual of the 2-grid is obtained as follows. The open interval between any two grid points (whether or not they belong to the same grid) is assigned an ordered pair of integers, (k_1, k_2), where the interval lies between grid points k_1 and $k_1 + 1$ of grid 1 and between grid points k_2 and $k_2 + 1$ of grid 2. The dual then maps the open interval into the point

$$x = k_1 L + k_2 S \; ,$$

which is a point in the 1D quasicrystal. A study of Fig. 3 reveals that this construction is identical with direct projection using the wider strip (projecting lower right-hand vertices of unit cells through which the projection line passes). The dual takes the place of identifying lower right-hand corner vertices and projecting. This result carries over a higher dimensions: *The grid projection, direction projection, and GDM for periodic Ngrids produce the identical structures*. As in one dimension, the GDM with quasiperiodic instead of periodic grids produces quasicrystals that cannot be obtained by projections from periodic lattices.

IV. TWO-DIMENSIONAL PENTAGONAL QUASICRYSTALS

In this section we shall extend the concepts discussed for 1D quasicrystals to the case of 2D pentagonal quasicrystals, both for intrinsic interest and as preparation for the more subtle case of 3D icosahedral quasicrystals. Several new features appear that were absent in the 1D case, due principally to the relation between the orientational symmetry (which has no analogue in one dimension) and the quasiperiodicity.

As mentioned above, the pentagonal quasicrystal can be described in terms of unit cells that repeat quasiperiodically throughout the structure. Many alternative sets of unit-cell shapes with different numbers of elements can be used. The simplest choice is a set of two unit cells consisting of a fat and skinny rhombus (see Fig. 4). The rhombic unit-cell packings for pentagonal quasicrystals can be obtained by the 2D analogue of the matching and deflation rules, grid projections, direct projections, or GDM. In two dimensions the special Penrose local iso-
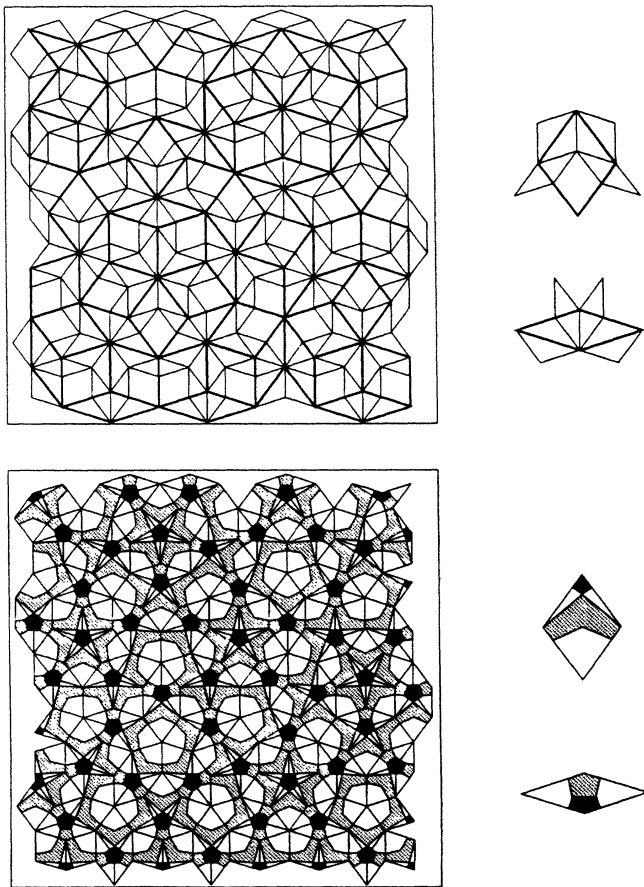
FIG. 4. Two simple decorations of a portion of a Penrose tiling. Top: The deflation decoration. The original tiling (heavy lines) has been decorated as shown at right to form another Penrose tiling (lighter lines). Bottom: A decoration that can be used to enforce the matching rules. According to the matching rules, a pair of tiles can join along an edge only if the strip decorations match across the interface.

morphism (PLI) class can be obtained by any of these methods.

The GDM produces the widest class of quasicrystal structures with pentagonal orientational symmetry. The general approach is to construct a 5-grid and then generate its dual. The simplest cases to construct and analyze are periodic pentagrids (periodic, linear 5-grids) and quasiperiodic pentagrids (quasiperiodic, linear 5-grids) as defined in Sec. II. In either case, the 5-grids are composed of straight lines oriented normal to one of the five pentagonal star vectors,

$$e_n = (\cos(2\pi n/5), \sin(2\pi n/5)) .$$

The angle of intersection between any two grids is either $\pi/5$ or $2\pi/5$; the duals to the intersection points correspond to skinny and fat rhombuses, respectively.

A. Local isomorphism

Given two tilings with pentagonal orientational symmetry, the same unit-cell shapes, and the same quasiperiodicity, several relations between them are possible. One may simply be a pure translation of the other, in which case we say the two are *equivalent*. Alternatively, the two may be completely different on all scales, containing different local configurations of cells. Such tilings are generally easy to distinguish visually. (See Fig. 1.) It is also possible for two tilings to differ in their global structure, but to be indistinguishable on the basis of any finite regions they contain, i.e., any finite region in either tiling exists somewhere in the other. Two tilings related in this way are said to be *locally isomorphic*. The precise definition of local ismorphism in two dimensions is as follows.

Definition: Two *tilings* are *locally isomorphic* if and only if given any point P in either tiling and any finite distance d, there exists a pure translation of the other tiling that causes the two to coincide everywhere in a circle of diameter d about P.

Definition: Two N-grids are *locally isomorphic* if and only if their dual tilings are locally isomorphic.

Note that this definition is somewhat more restrictive than that used in paper I in that two tilings that are related by a rotation or inversion may not be locally isomorphic. This more restrictive definition will simplify the discussion in Secs. IV and V.[2] This restriction does not affect our discussion because the PLI class tilings we will study are locally isomorphic (under the more restrictive definition) to their inversions. Note also that two tilings are not locally isomorphic if there exists a single finite region of one that is not found in the other. Two tilings that are both locally isomorphic to a third tiling are locally isomorphic to one another. Thus, the set of all tilings can be divided into local isomorphism (LI) classes, where two tilings in the same LI class if an only if they are locally isomorphic.

Definition: Two N-grids are *topologically equivalent* if the grid curves of one N-grid can be continuously distorted to form the other N-grid without any intersection crossing any curve.

The duals of two two topologically equivalent N-grids are identical up to translations and rotations. Given a quasicrystal tiling, we can form its *skeleton* which is both an N-grid and a quasilattice. The dual of the skeleton is the tiling itself. In practice, however, it is difficult to form the skeletons or tilings directly, and we must content ourselves with the study of a subset of skeletons that are topologically equivalent to linear N-grids. These linear N-grids can be generated easily and their duals taken to form quasicrystal tilings.

B. Grid projections, direct projections and duals of periodic pentagrids

A grid projection or direct projection from a five-dimensional periodic hypercubic lattice to two dimensions, and the dual of a periodic pentagrid are different techniques for obtaining exactly the same pentagonal quasicrystal packings of rhombic unit cells. The fact that the original Penrose tilings can all be obtained by duals to *special* periodic pentagrids suggests the possibility of obtaining the same tilings by projections.[9] In this section we will discuss some general properties of periodic pentagrids and their duals. In a later subsection, we will specialize to the PLI class.

Unlike their analogues in one dimension, the projection techniques generate an infinite number of LI classes, although still only a small subset of the tilings generated by the GDM. It is equivalent to analyze the LI classes of the tilings or of the pentagrids whose duals generate the tilings. (Two periodic pentagrids are locally isomorphic if and only if their dual tilings are locally isomorphic.) Recall from Sec. II, that a periodic pentagrid can be designated by its five free (grid shift) parameters $\{\gamma_n\}$. There is a simple condition on the $\{\gamma_n\}$ for locally isomorphic pentagrids:

Theorem 4.1. Two pentagrids, $\{\gamma_n\}$ and $\{\gamma_n'\}$, are locally isomorphic if and only if

$$\sum_{n=0}^{4} \gamma_n - \sum_{n=0}^{4} \gamma_n' = m, \quad m \in \mathbb{Z} . \tag{15}$$

A proof of this theorem is given in Appendix A.

We thus have a continuum of tiling classes generated by pentagrids, with each class characterized by the fractional part of $\sum_{n=0}^{4} \gamma_n$. de Bruijn has shown that the special choice, $\sum_{n=0}^{4} \gamma_n = 0$, corresponds to the set of pentagrids whose duals correspond to the PLI class. These are precisely the tilings which are obtained by Penrose using the *matching and deflation rule* approach. We will discuss the special properties of these pentagrids and the tilings shortly. In general, though, $\sum \gamma_n \neq 0$ and the tilings that are generated do not obey the Penrose matching rules.

To see that the tilings generated from periodic pentagrids always have quasiperiodic translational order we examine a single line in any grid, say grid 0, and its intersections with the other four grids; see Fig. 5. [We number the grids, $n = 0, 1, \ldots, 4$, where the nth grid consists of lines normal to $e_n = (\cos(2\pi n/5), \sin(2\pi n/5))$. We choose the periodic interval between grid lines to equal unity.] Grids 1 and 4 each intersect grid 0 with intersection angle $2\pi/5$ (we will call these type I intersections)

and the intersection points of each are spaced periodically along grid 0 with period $\csc(2\pi/5)$. The dual of a type I intersection is a fat rhombus whose orientation is different for grid 1 and grid 4. Note that along grid 0 the intersections with grid 1 alternate with those of grid 4. Grids 2 and 3 intersect grid 0 with intersection angle $\pi/5$ (type II intersections) and the intersection points are spaced periodically along grid 0 with period $\csc(\pi/5)$. The dual of a type II intersection is a skinny rhombus with two possible orientations. Since $\csc(\pi/5)/\csc(2\pi/5) = \tau$ is irrational the sequence of type I and II intersections along the grid 0 line is quasiperiodic. This means, of course, that the sequence of rhombic cells dual to these intersections is quasiperiodic. Since the widths of the different types of cells are different, the y coordinates [recall $e_0 = (1,0)$] of their vertices also form a quasiperiodic sequence.

This analysis brings to light some other features common to all duals of *periodic* pentagrids which are not necessarily true for quasiperiodic pentagrids. The fact that the grid 1 and 4 (or grid 2 and 3) intersections with grid 0 must alternate means that two consecutive intersections are never completely identical. It is therefore impossible for adjacent cells in the dual tiling to have both the same shape and the same orientation. Furthermore, type II intersections are τ times as dense along any line in the N-grid as type I intersections. This implies that the ratio
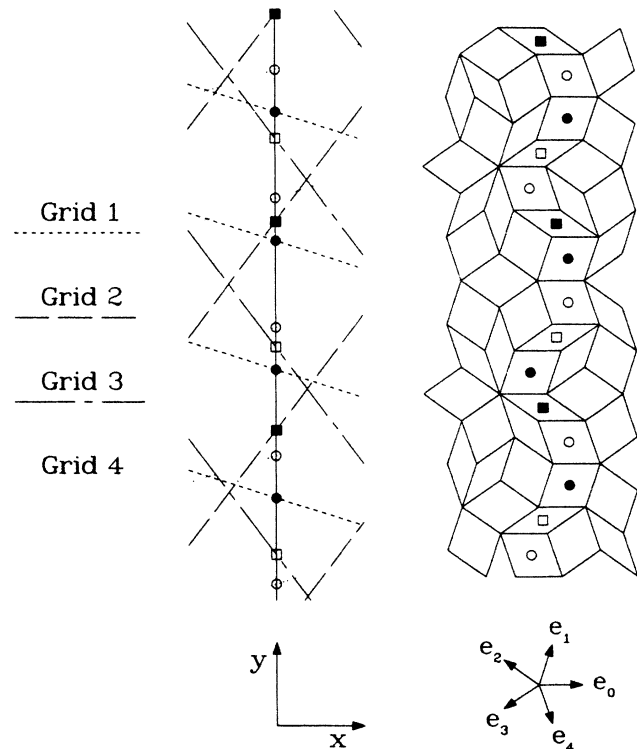

FIG. 5. Illustration of the GDM applied to a periodic pentagrid. Attention is focused on a single (vertical) line belonging to grid 0. The tiles marked on the right are dual to their similarly marked counterparts in the pentagrid on the left. Circles are used for type I intersections and squares for type II (see Sec. IV B). The y coordinates of the vertices of the marked tiles form a quasiperiodic sequence.

of the number of fat tiles to skinny tiles in the dual of any periodic pentagrid is τ:1.

A pentagrid (or quasiperiodic pentagrid) in which three or more grid lines intersect at a point is said to be *singular*.[9] For periodic grids, singular pentagrids represent a degeneracy of two or more tilings. To obtain the individual tilings, the singularity must be *resolved* in all possible ways by shifting the grids (the γ_n's) infinitesimally with respect to one another in all possible directions keeping $\sum_n \gamma_n$ fixed. If three lines intersect in a single point, for example, one of them can be shifted an infinitesimal amount in either of two directions to yield two different triangular configurations of intersections. Infinitesimal shifts in the other two lines do not result in any more topologically distinct configurations of intersections. The duals of the two configurations correspond to different tilings. We therefore say that a periodic pentagrid containing one *threefold singularity* yields two tilings.

For periodic pentagrids the existence of a single threefold singularity implies the existence of an infinite number of them, all collinear. A shift that resolves any one of these, however, determines a unique resolution of all of them, so that the pentagrid still gives rise to only two distinct tilings. For our present purposes the singular periodic pentagrids are of no special interest. Singular quasiperiodic hexagrids will prove to be very interesting for the 3D icosahedral case, though.

C. Duals of quasiperiodic pentagrids

For reasons that will become clearer when we discuss 3D icosahedral quasicrystal packings, we wish to discuss the LI classification of quasiperiodic pentagrids in addition to periodic pentagrids. The great variety of possible quasiperiodic grids makes it difficult to obtain a complete classification of quasiperiodic pentagrids and their duals. We will restrict ourselves almost exclusively to the case of quasiperiodic pentagrids that are composed of grids based on the Fibonacci sequence with two spacings, L and S, in the ratio τ:1. These are the Fibonacci pentagrids $\{\alpha_n, \beta_n\}$ with $\rho = \sigma = \tau$. These quasiperiodic pentagrids are not only linear 5-grids, but the set of grid intersection points also satisfies the criteria for a quasilattice. In particular, there is a minimum distance, $r > 0$, between intersection points. As we shall see, for special choices of the free parameters, the Fibonacci pentagrid and the Ammann quasilattice (see paper I and below) are identical.

In Fig. 1, we exhibit characteristic portions of a Penrose tiling, a tiling dual to a Fibonacci pentagrid, and a tiling dual to a non-Fibonacci pentagrid. The Penrose tiling can be obtained as a dual to a periodic or a Fibonacci pentagrid for special choices of parameters. Figure 1(b) is an example which can be obtained via Fibonacci pentagrids but not via periodic pentagrids. From the figure, it is clear that the various tilings belong to different LI classes. Certain configurations of tiles appear in each that do not appear in the others. Note that the dual to the Fibonacci pentagrid shown in Fig. 1(b) does contain pairs of adjacent rhombuses of the same type and orientation and that the dual to the non-Fibonacci pentagrid contains longer chains of this type.

As with periodic pentagrids, Fibonacci pentagrids can be subdivided into LI classes. It is useful to further subdivide them into local congruence classes:

Definition: Two Fibonacci pentagrids are *locally congruent* if and only if as *quasilattices* they are locally isomorphic; that is, the pentagrids (not just the dual tilings) can be made to coincide exactly out to arbitrarily large finite distances about any point in either pentagrid.

The fact that a Fibonacci pentagrid has a minimum separation between intersection points means that a small shift ($\ll r$) of a single grid does not change the topology of intersections and so the original and shifted pentagrids are locally isomorphic. However, the small shift will change the shapes of the open regions between grid lines. Thus, the shifted pentagrid is not locally congruent to the original.

Before stating the local congruence theorem for Fibonacci pentagrids, it is useful to define two types of equivalence transformations of the α_n's and β_n's. These transformations are extensions to two dimensions of the transformations discussed for 1D quasicrystals (see Sec. III).

(1) The *umklapp* transformation:

$$\alpha_n \rightarrow \alpha_n + p_n + \frac{1}{\tau} q_n, \quad \beta_n \rightarrow \beta_n - q_n + \frac{1}{\tau} p_n , \qquad (16)$$

where p_n and q_n are integers. Under such a transformation we find

$$x_{nN} \rightarrow N + \alpha + p_n + \frac{1}{\tau} \left| \frac{N}{\tau} + \beta + \frac{1}{\tau} p_n \right|$$

$$\rightarrow x_{n(N+p)} . \qquad (17)$$

This transformation merely re-indexes the lines in each grid. We also will use the term "umklapp" as a verb so that we can speak of umklapping a grid by a number of the form $p + q/\tau$ (for $p, q \in Z$) as a transformation between $(\alpha + p + q/\tau, \beta)$ and $(\alpha, \beta - q + p/\tau)$; this transformation leaves the structure completely unchanged.

(2) The β *translation*:

$$\beta_n \rightarrow \beta_n + z \cdot e_{\langle 3n \rangle} ,$$

where

$$z = \left[\frac{m_1 + m_2/\tau}{\cos(2\pi/5)}, \frac{m_3 + m_4/\tau}{\sin(2\pi/5)} \right], \quad m_i \in Z \qquad (18)$$

and $\langle 3n \rangle$ means $\mathrm{mod}_5(3n)$. This transformation is equivalent to an umklapp followed by a pure translation. (The proof of this is given in Appendix B.) Note that although we have restricted z to a special set of vectors, this set is dense in the plane (the m's are all independent).

These two types of transformation of a Fibonacci pentagrid (as well as pure translations) yield pentagrids that are equivalent to the original. The criteria for local

congruence are, however, a bit weaker than for equivalence.

Theorem 4.2. Two Fibonacci pentagrids $\{\alpha_n,\beta_n\}$ and $\{\delta_n,\gamma_n\}$ are composed of grids with directions

$$\mathbf{e}_n = (\cos(2\pi n/5),\ \sin(2\pi n/5))$$

and line positions given by

$$x_{nN} = N + \alpha_n + \frac{1}{\tau}\left[\frac{N}{\tau} + \beta_n\right]$$

and

$$x'_{nN} = N + \delta_n + \frac{1}{\tau}\left[\frac{N}{\tau} + \gamma_n\right].$$

$\{\alpha_n,\beta_n\}$ is locally congruent to $\{\delta_n,\gamma_n\}$ if and only if there exist integers p_n, q_n and vectors $\mathbf{u},\mathbf{v}$ (not necessarily vectors corresponding to β translations) such that

$$\Delta\alpha_n \equiv \alpha_n - \delta_n = \mathbf{u}\cdot\mathbf{e}_n + p_n + \frac{1}{\tau}q_n ,$$

$$\Delta\beta_n \equiv \beta_n - \gamma_n = \mathbf{v}\cdot\mathbf{e}_{\langle 3n\rangle} - q_n + \frac{1}{\tau}p_n . \tag{19}$$

Proof: By successively applying β translations, umklapps and pure translations to $\{\delta_n,\gamma_n\}$ we can make $\Delta\alpha_n$ zero and $\Delta\beta_n$ arbitrarily close to zero simultaneously. First we apply a β translation to $\{\delta_n,\gamma_n\}$ with the vector $\mathbf{z}$ chosen as close as desired to $\mathbf{v}$. In this way we can come arbitrarily close to eliminating the $\mathbf{v}\cdot\mathbf{e}_{\langle 3n\rangle}$ term from $\Delta\beta_n$. Next we umklapp each grid in $\{\delta_n,\gamma_n\}$ to eliminate all of the p_n's and q_n's from $\Delta\alpha_n$ and $\Delta\beta_n$. Finally, we can make $\Delta\alpha_n$ zero by placing the origin for $\{\delta_n,\gamma_n\}$ at the tip of $\mathbf{u}$. We denote the new values of δ_n and γ_n by δ'_n and γ'_n. $\{\delta'_n,\gamma'_n\}$ is equivalent (not just locally isomorphic) to $\{\delta_n,\gamma_n\}$.

Since $\alpha_n = \delta'_n$ the $N=0$ lines of $\{\alpha_n,\beta_n\}$ and $\{\delta'_n,\gamma'_n\}$ coincide exactly. Now the difference between β_n and γ'_n affects only those lines in the quasilattice that correspond to an N for which $N/\tau+\beta_n$ and $N/\tau+\gamma'_n$ have different integer parts. This can be made to occur only for arbitrarily large values of N since γ'_n can be made arbitrarily close to β_n for all n simultaneously. Thus each grid of $\{\delta'_n,\gamma'_n\}$ (and, therefore, $\{\delta_n,\gamma_n\}$) can be made to coincide exactly with its partner in $\{\alpha_n,\beta_n\}$ out to arbitrarily large distances about the $N=0$ line. Since by umklapping we can arrange for the $N=0$ lines to be anywhere in $\{\alpha_n,\beta_n\}$ and since the same proof can be repeated with the roles of $\{\alpha_n,\beta_n\}$ and $\{\delta_n,\gamma_n\}$ interchanged, $\{\delta'_n,\gamma'_n\}$ is locally congruent to $\{\alpha_n,\beta_n\}$.

We take it as self-evident that no transformations of the α's other than umklapps and pure translations are equivalence transformations. It is also evident from the proof in Appendix B that no transformations of the β's other than umklapps and β translations are equivalent transformations. The conditions of Eqs. (19) are thus necessary for two quasilattices to be locally congruent.

We will show in the next subsections that there exists a special subset (special choices of $\{\alpha_n,\beta_n\}$) of Fibonacci pentagrids in the PLI class, called Ammann quasilattices, which can be obtained directly from the tilings via a sim-

ple decoration of each tile shape. As a result, since a Penrose tiling and its deflation are locally isomorphic (that is, the tilings can be made to coincide out to arbitrarily large finite distances), the Ammann quasilattice which decorates the tiling and its "deflation" must share this property. That is, the Ammann quasilattices must be locally congruent to their deflations (the formal definition of the deflation of a pentagrid is given in Sec. IV B). The other Fibonacci pentagrids in the PLI class are trivially related to the Ammann quasilattices by small shifts ($\ll r$) of the grids. We will make use of this deflation property in determining the $\{\alpha_n,\beta_n\}$ appropriate to an Ammann quasilattice. Once we have identified one Fibonacci pentagrid in the PLI class and the dual tiling has been constructed, all of the tilings locally isomorphic to the dual can be obtained by first making a local congruence transformation [Eqs. (19)] on $\{\alpha_n,\beta_n\}$ and then taking the dual. Thus, to identify the entire PLI class of tilings it is sufficient to determine the values of α_n and β_n corresponding to any single Ammann quasilattice. The PLI class tiling is then obtained by taking the dual of the Ammann quasilattice.

We show in subsequent sections that the PLI class can be generated by the Fibonacci pentagrids (Ammann quasilattices) given by

$$\alpha_n = \frac{6\tau-1}{2(\tau+2)}, \quad \beta_n = \frac{-2}{\tau+2} \quad \text{for all } n . \tag{20}$$

The fact that the PLI class can be generated as a dual to either a periodic pentagrid or a Fibonacci pentagrid is a coincidence. For the particular choice of parameters appropriate to the PLI class, the two pentagrids happen to be topologically equivalent. This topological equivalence does not occur for the PLI class in the 3D icosahedral packings.

Reasoning quite similar to that used for the periodic pentagrids reveals that duals of Fibonacci pentagrids have a ratio of fat to skinny rhombuses equal to $\tau{:}1$. In contrast to the duals of periodic pentagrids, the duals of some Fibonacci pentagrids contain adjacent rhombuses of the same type and orientation. For the Fibonacci pentagrid, intersections of the same type can succeed each other along a given grid line because there are two different spacing lengths within each grid. Since the ratio of spacings is less than 2:1, however, it is impossible to have three consecutive intersections of the same type and thus no dual tiling contains a string of more than two adjacent rhombuses of the same type and orientation. Of course by choosing ρ small and σ large, we can arrange to have duals of more general quasiperiodic pentagrids with arbitrarily long chains of this type. (See Fig. 1.)

This simple analysis clearly demonstrates, then, that the set of duals to quasiperiodic pentagrids, and Fibonacci pentagrids in particular, contain tilings that cannot be realized as duals to periodic pentagrids. Also, the sets of duals to quasiperiodic pentagrids and periodic pentagrids have a nonempty intersection since both contain the PLI class. At the time of this writing we have not determined the full extent to which the two sets overlap.

D. Penrose tilings: The 2D pentagonal PLI class

1. The special properties of Penrose tilings

Of all the rhombic unit cell structures that can be generated as duals to pentagrids or pentagonal quasilattices, the *original Penrose tilings*—which comprise the pentagonal PLI class—are surely the most intriguing. They have several elegant properties that the elements of other classes do not share. The three most important properties of the PLI class (PP1—PP3) are the following.

PP1: There exist a set of *simple* local matching rules for the tiles that force a tiling in the PLI class.

PP2: There exist *simple* inflation and deflation rules (self-similarity transformations).

PP3: There exists a *simple* decoration of the tiles in a Penrose tiling which forms a linear, quasiperiodic (Fibonacci) pentagrid (which we have termed an Ammann quasilattice).

These properties are all interrelated, the key being PP3. In general, a *decoration* is any pattern obtained by a rule for marking the tiles in a tesselation. A *simple* decoration of a tiling is a pattern formed by marking the tiles such that all tiles of the same type are marked in exactly the same way. A *context dependent* decoration of a tiling is a pattern formed by marking tiles such that the marking depends both on the tile type and on the local configuration of tiles (within some finite radius) about the tile position in the tesselation.

For PP1 there exist rules that constrain the way two tiles can adjoin edge on edge (and vertex to vertex) such that the only tilings that fill the plane and that are consistent with the rules are quasicrystal tilings in the PLI class. These *matching rules* can be enforced by introducing a set of bumps and nicks on every fat tile and a set on every skinny tile (the same bumps and nicks appear on each tile of a given type). Alternatively, the matching rules can be enforced simply by decorating the tiles with stripes, say, and requiring the stripes to match along the edges of adjacent tiles. (See Fig. 4.)

We say the rules are *simple* because each fat tile has the same matching rule and each skinny tile has the same matching rule. (One can imagine context dependent matching rules in which there are two or more different fat and/or skinny tiles with different matching rules.)

There are an infinite variety of tilings consistent with the matching rules corresponding to the different elements of the PLI class. The matching rules are such that it is possible to begin to construct a tiling consistent with the matching rules at each stage, but then discover that the tiling cannot be completed. That is, the rules are only local and do not guarantee a plane-filling tiling. What is guaranteed is that it is possible to construct a plane-filling tiling and that such a tiling must be a Penrose tiling. Changing a tiling that cannot be completed into one that can be may require the rearrangement of only a few tiles, but it may be necessary to rearrange arbitrarily large portions of the tiling.

The possibility of forcing a quasicrystal unit cell struc-

ture with local matching rules may be an important factor in the growth of some quasicrystals. A possible scenario for some atomic systems is that atomic clusters form which can pack together only in special ways, corresponding to a physical manifestation of the matching rules. In Fig. 6, we illustrate an example of an "atomic decoration" of the Penrose tiling. Each fat rhombus has been decorated with the same atomic cluster and each skinny rhombus has been decorated with a different cluster (we have superimposed a portion of the original tiling in the corner of the figure). If the two clusters were forced by local "bonding" rules, say, an atomic configuration of the type shown in the figure might be energetically favorable. Even under these conditions, it is likely that, given only local matching rules, the structure could not be grown perfectly.[26] Defects would form where clusters could not fill a region consistent with the matching rules (in the same way that a tiling built from local matching rules may not be able to fill the plane). The defects, however, can be reduced to point defects, according to the theorem of Conway which states that any untileable region can be reduced to a small finite area (a decapod).[12] Thus, such defects would not be more costly energetically than a dislocation, say, and would not suppress quasicrystal growth. (In three dimensions, the analogous defect can be reduced to a line defect.)

For PP2 we say that the deflation rule for the PLI class is *simple* because it corresponds to a *simple decoration* of the tiles. That is, given a Penrose tiling, a decoration exists with the property that the decoration markings themselves form a Penrose tiling consisting of tiles of side
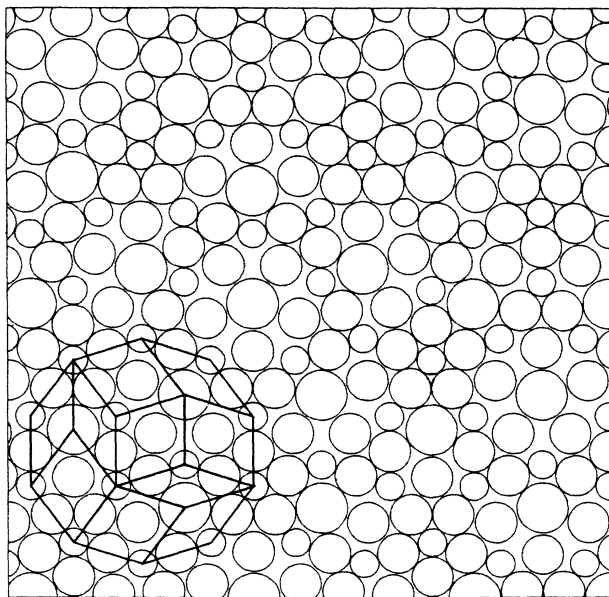

FIG. 6. Example of an atomic decoration of a Penrose tiling that is in one-to-one correspondence with the matching rules. A small portion of the tiling has been superimposed so that the decoration is more readily visible. This picture is meant to convey some idea of the kind of structure that can be produced by simple decoration. It is not to be taken as a realistic model for a physical material.

length $1/\tau$ times the side length of the original tiles. This decoration is the same for all Penrose tilings and is depicted in Fig. 4. We call the pattern of small tiles the *unscaled deflation* of the original tiling. The *deflation* of a tiling (not unscaled) refers to the same pattern, but scaled up by τ so that its constituent tiles are the same size as those in the original.

Two aspects of this deflation procedure are unusual: Although deflation procedures can be defined for many tilings, in all other known cases the decoration is context dependent (different fat tiles might be decorated differently, for example). Also, in the Penrose case the deflation of a pattern is locally isomorphic to the original.[11,12,15]

The inverse of deflation is called *inflation*. An unscaled inflation consists of tiles with side length τ times that of the original tiles. Rules can be formulated for the joining of tiles to form an inflation, although they are not as simple as the procedure for deflation. The existence of unambiguous inflation and deflation procedures forms the basis for many of the proofs of the unique properties of Penrose tilings.

For PP3 there is another simple decoration of a Penrose tiling that generates a linear, quasiperiodic (Fibonacci) pentagrid which we have termed an *Ammann quasilattice*.

Figure 7 depicts the decoration of the Penrose tiling, with the marking of individual tiles illustrated below.
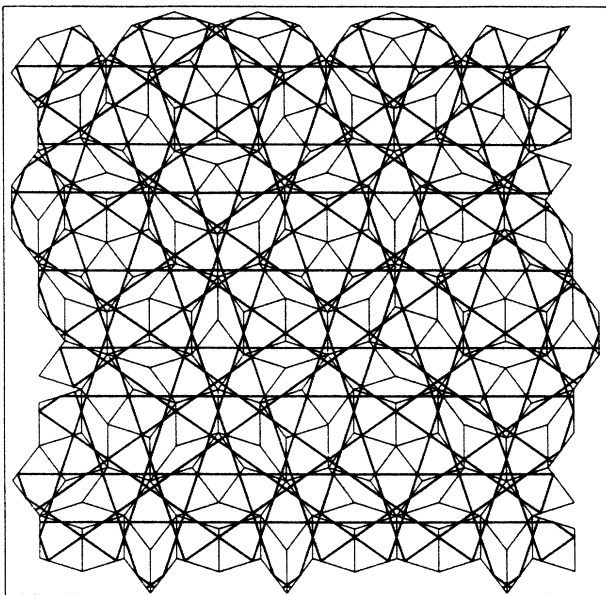
FIG. 7. Ammann line decoration of a portion of a Penrose tiling. The tiles have been decorated as shown at bottom to reveal the Ammann quasilattice associated with the tiling. The dual of this Ammann quasilattice is another Penrose tiling that is precisely the deflation of the one shown in this figure, according to the deflation rules shown in Fig. 4.

The proof that the decoration does indeed form a Fibonacci pentagrid makes use of the deflation procedure. By constructing a small portion of a tiling and using some simple geometry one can see that the ratio of spacings in the decoration is $\tau{:}1$. By deflating a few small portions and decorating the unscaled deflation in the same way one can derive a rule for the "deflation" of a decoration. The result is that the grids formed by the decoration can each be deflated independently according to the rule

$$L \rightarrow \frac{L}{2}S\frac{L}{2}, \quad S \rightarrow \frac{L}{2}\frac{L}{2} . \tag{21}$$

An unscaled deflation of a grid is depicted in Fig. 2. Now Eq. (21) is precisely the rule that generates a Fibonacci sequence of spacings. Since it can be applied in reverse an infinite number of times (corresponding to inflations of the tiling), the grids in the decoration must form a Fibonacci pentagrid.

Thus to each Penrose tiling there corresponds an Ammann quasilattice and there is a simple deflation procedure for this quasilattice that yields the Ammann quasilattice of the deflation of the tiling. Since the deflation of a Penrose tiling is locally isomorphic to the original and the Ammann quasilattice is obtained by the same decoration in both cases, *the deflation of an Ammann quasilattice must be locally congruent to the original.*

A set of matching and deflation rules for the tiles can be derived directly from the Ammann quasilattice (which is why we regard it as so fundamental to the PLI class). The decoration of the tiles in Fig. 7 can be regarded as a matching rule, the rule being that two tiles are only allowed to match edge on edge if all the decoration lines are continued linearly across the interface. This decoration and rule is slightly different from that given in Fig. 4, but it also forces tilings that fill the plane to be of the PLI class.

Another remarkable property of the Ammann quasilattice is that it contains the information necessary to construct the deflation rules: *The dual of the Ammann quasilattice, now treated as a quasiperiodic pentagrid, is the deflation of its associated tiling.* To see this one need only inspect the decorations that yield the Ammann quasilattice and the deflation of a tiling. To each intersection in the Ammann decoration there corresponds a rhombus of the appropriate type and orientation in the deflation decoration.

2. Penrose tilings as duals of Ammann quasilattices

As we have seen, the dual of an Ammann quasilattice, which is a case of a Fibonnaci pentagrid (see Sec. IV C), is a Penrose tiling. Our goal in this subsection is to derive the special choices of $\{\alpha_n,\beta_n\}$ [given in Eq. (20)] that correspond to Ammann quasilattices. A special property that allows us to identify these quasilattices is that they are locally congruent to their deflations (see Sec. IV A). The *deflation* of a general Fibonacci pentagrid is now defined to be the pentagrid obtained by deflating each of its five component (Fibonacci) grids according to the deflation rule for a 1D Fibonacci sequence, as shown in Fig. 2.

We denote the deflation of $\{\alpha_n,\beta_n\}$ by $\{\alpha_n^*,\beta_n^*\}$. After

determining the relations between α_n^* and α_n and between β_n^* and β_n we can enforce the condition that $\{\alpha_n^*,\beta_n^*\}$ be locally isomorphic to $\{\alpha_n,\beta_n\}$ to single out the Ammann quasilattices.

The following two theorems show that the set of Fibonacci pentagrids that are locally congruent to their deflations is closed under deflation and that such pentagrids are locally congruent to each other.

Theorem 4.3. $\{\alpha_n^*,\beta_n^*\}$ is locally isomorphic to $\{\alpha_n^{**},\beta_n^{**}\}$ if $\{\alpha_n,\beta_n\}$ is locally isomorphic to $\{\alpha_n^*,\beta_n^*\}$.

Theorem 4.4. If $\{\alpha_n,\beta_n\}$ is locally isomorphic to $\{\alpha_n^*,\beta_n^*\}$ and $\{\delta_n,\gamma_n\}$ is locally isomorphic to $\{\delta_n^*,\gamma_n^*\}$, then $\{\alpha_n,\beta_n\}$ is locally isomorphic to $\{\delta_n,\gamma_n\}$.

(The proofs are conceptually trivial, but tedious, and are given in Appendix C.)

From these theorems we conclude that the set of all Fibonacci pentagrids which are locally congruent to their deflations can be obtained by first finding one such $\{\alpha_n,\beta_n\}$ and then making all possible local congruence transformations according to Eqs. (19). We know that this set must be precisely the Ammann quasilattices since we have already shown by other means (see Sec. IV A) that they are locally congruent to their deflations. All that remains is to find some specific choice of $\{\alpha_n,\beta_n\}$ in this set.

The easiest example to find is one of the cases that has a center of pentagonal point symmetry. Clearly, such a pattern can be specified by $\{\alpha_n,\beta_n\}$ with $\alpha_n=\alpha$, $\beta_n=\beta$, for all n. We will use $\Delta\alpha$ and $\Delta\beta$ for $\alpha-\alpha^*$ and $\beta-\beta^*$. The local congruence conditions of Eqs. (19) are then equivalent to the following three (see Appendix D):

$$\Delta\alpha=\frac{1}{5}\left[P+\frac{1}{\tau}Q\right],$$

$$\Delta\beta=\frac{1}{5}\left[-Q+\frac{1}{\tau}P\right], \tag{22}$$

and

$$P+2Q=5k$$

for some integers P, Q, and k. Furthermore, it is always possible to umklapp α and β so as to make $-2\leq P$, $Q\leq2$. These conditions can be satisfied by four (P,Q) pairs only: $(1,2)$, $(2,-1)$, $(-1,-2)$, and $(-2,1)$. [Although $(0,0)$ appears to work, it yields $\beta=0$, which is of the form $k+l/\tau$ for some integers k and l; the correct treatment of this case shows that it is not locally congruent to its deflation and its dual is not a Penrose tiling.] The values of α and β that correspond to an allowed (P,Q) can be found using the deflation equations, Eqs. (10) and (11); the answer for $(1,2)$ is

$$\alpha=\frac{6\tau-1}{2(\tau+2)} \text{ and } \beta=\frac{-2}{\tau+2}.$$

The dual to this pentagrid is one of the special Penrose tilings with a center of symmetry (which comprise a subset of measure zero among all possible Penrose tilings). All other Penrose tilings can be generated by first transforming $\{\alpha_n,\beta_n\}$ according to Eqs. (19) and then taking the dual.

For completeness we mention also that there is a rela-

tionship between the γ_n's of the periodic pentagrid and the α_n's and β_n's of the Fibonacci pentagrid for the special case where both duals correspond to the same tiling in the PLI class. The relation is

$$\gamma_n=\frac{\alpha_n+(1/\tau)(\beta_n-\frac{1}{2})}{1+1/\tau^2}. \tag{23}$$

Note that a shift of γ_n by an integer (where the periodic grid spacing is unity) leaves the periodic pentagrid and its dual unchanged; an umklapp (see Sec. III A) leaves the quasiperiodic pentagrid unchanged and shifts the expression on the right-hand side by an integer. This relation was derived by comparing the deflation rule for pentagrids given by de Bruijn[9] and the deflation rule for $\{\alpha_n,\beta_n\}$.

A further word should be said about tilings that do not belong in the PLI class and the value of studying the PLI class. It is difficult to distinguish other tilings from those in the PLI class on the basis of their diffraction properties; they produce peaks at the same positions, albeit with some minor variations in intensities (see paper I). We have argued that they do not have simple matching rules and so it seems difficult to "design" a physical system that is forced to conform to one of these cases. For the case of I-Al-Mn we have no reason to believe that the quasicrystals belong to the PLI class. Nevertheless they must belong to some LI class and it is at least useful to understand the properties that are shared by elements of a single class since these have physical consequences (such as invariance of the diffraction pattern and peak intensities under a LI transformation). At the very least, the PLI class is of special interest to physicists because it is possible to make use of the closer relation between the Penrose tilings and their associated Ammann quasilattices in computations. The fact that the Ammann quasilattice is itself a decoration of the inflation of those tilings may provide us, for example, with a way to specify the positions of a single type of tile, and therefore may be useful in associating form factors in diffraction calculations. We do not know how to do this for an arbitrary GDM tiling.

V. ICOSAHEDRAL QUASICRYSTALS

In this section we discuss the construction of icosahedral quasicrystal packings of unit cells and present the detailed construction of the PLI class of icosahedral packings. These special packings are characterized by simple matching and deflation rules and an underlying quasilattice of quasiperiodically spaced planes analogous to the 2D Ammann quasilattice. For various reasons, this construction is more subtle than the 2D analogue. Nevertheless, it can be approached in an analogous way and our treatment here relies heavily on the concepts that have been defined and illustrated for the simpler 1D and 2D cases.

The 3D icosahedral analogue of the 2D rhombic unit cells are the two rhombohedra shown in Fig. 8. In the icosahedral packings the different rhombohedra are packed face to face and vertex to vertex. As in 1D or 2D, the 3D icosahedral packings can be generated by the matching and deflation rules, the grid projections, the

direct projections, or the GDM. For 3D, though, the PLI class cannot be generated by the grid projection or direct projection methods (although it may be possible to generalize these methods to generate the PLI class). The most straightforward way of describing the construction of the 3D icosahedral PLI class is via the GDM.

The set of star vectors for the icosahedral vertex model is

$$\mathbf{e}_n = ((2/\sqrt{5})\cos(2\pi n/5), (2/\sqrt{5})\sin(2\pi n/5), 1/\sqrt{5})$$

for $n = 0, 1, \ldots, 4$ and $\mathbf{e}_5 = (0,0,1)$. Two types of nonsingular intersections arise in periodic and quasiperiodic hexagrids based on this star, whose duals are the two types of rhombohedra shown in Fig. 8. Each face of these rhombohedra is a rhombus with acute angles $\arccos(1/\sqrt{5})$. The prolate rhombohedron has edges parallel to the triplet of vectors $(\mathbf{e}_5, \mathbf{e}_0, \mathbf{e}_1)$ or some triplet with the same intersection angles. The other, the oblate one, is based on a triplet of the type $(\mathbf{e}_5, \mathbf{e}_0, \mathbf{e}_2)$.

A. Grid projections, direct projections and the GDM for periodic hexagrids

Packings corresponding to duals of periodic hexagrids have been discussed already by several authors. They are precisely the same packings that are generated by the grid or direct projection techniques from six-dimensional hypercubic lattices. The direct projection technique has proven helpful in certain aspects of the analysis of these packings (e.g., in computing the densities of various local unit cell configurations). We wish, however, to emphasize the following theorem.

Theorem 5.1. All duals to (nonsingular) periodic hexagrids are in the same local isomorphism class.

Proof: The proof of this theorem is quite similar to that of Theorem 4.1 (Appendix A). Consider any two
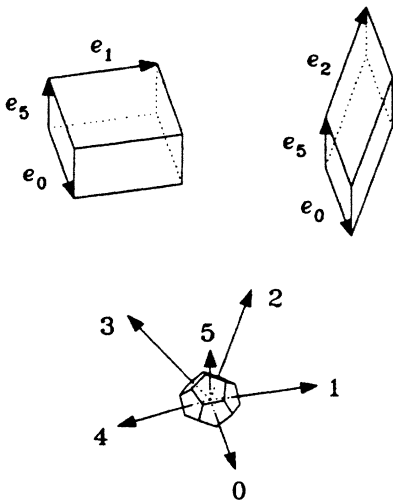

FIG. 8. Two types of rhombohedra that arise naturally in icosahedral quasicrystal packings and the star of vectors chosen for the analysis of the vertex model. The prolate rhombohedron (left) is based on a triplet of the form $(\mathbf{e}_5, \mathbf{e}_0, \mathbf{e}_1)$, the oblate on a triplet of the form $(\mathbf{e}_5, \mathbf{e}_0, \mathbf{e}_2)$.

hexagrids, $\{\gamma_n\}$ and $\{\gamma_n'\}$. Each is formed from two overlapping incommensurate periodic lattices which we will designate Λ_1 and Λ_2 in $\{\gamma_n\}$, and Λ_1' and Λ_2' in $\{\gamma_n'\}$. Λ_1 and Λ_1' are formed by grids in the $(\mathbf{e}_5, \mathbf{e}_0, \mathbf{e}_1)$ directions; Λ_2 and Λ_2' are formed by grids in the $(\mathbf{e}_2, \mathbf{e}_3, \mathbf{e}_4)$ directions. Without loss of generality, let the origin, Ω, of $\{\gamma_n\}$ be any lattice point in Λ_1. Let $\mathbf{v}$ be the displacement from Ω to any lattice point in Λ_2. The hexagrid $\{\gamma_n\}$ is completely determined by choosing Ω and $\mathbf{v}$. (This is slightly different from the 2D case where the pentagrid is formed from two periodic lattices composed of two grids each plus an *extra* grid. To determine the pentagrid, not only are the analogues of Ω and $\mathbf{v}$ required, but also the relative position of the extra grid.) Now, we can translate any lattice point in Λ_1' so that it overlaps Ω; then Λ_1' and Λ_1 will exactly overlap. Because Λ_1' and Λ_2' are two incommensurate periodic lattices, for any ϵ there exists a lattice point Ω' in Λ_1' and a lattice point R in Λ_2' such that their relative displacement, $\mathbf{z}$, has the property that $|\mathbf{z} - \mathbf{v}| < \epsilon$. By making ϵ arbitrarily small, and translating the associated Ω' to Ω, Λ_1' is guaranteed to exactly overlap Λ_1 and Λ_2' approaches arbitrarily close to Λ_2. As a result, duals to the hexagrids $\{\gamma_n\}$ and $\{\gamma_n'\}$ can be made to coincide exactly out to any finite distance. Thus, the hexagrids are locally isomorphic. (In two dimensions, it is not sufficient for the two pairs of periodic lattices to coincide to arbitrary accuracy; the relative position of the extra grid must also coincide. To ensure this, it is necessary that $\sum_n \gamma_n - \sum_n \gamma_n'$ be an integer.)

Theorem 5.1 suggests that it is important to study packings generated by techniques other than projection from hypercubic lattices in order to appreciate the full range of possible icosahedral quasicrystal structures. The duals of quasiperiodic hexagrids, for example, can contain long chains of identical rhombohedra and thus appear quite different from the projection packings on a local level. (See Fig. 1 for the 2D analogue.) The different possible local configurations of unit cells should be considered when trying to determine the atomic decoration of I-Al-Mn and related alloys. Furthermore, we shall see that the icosahedral packings in the PLI class cannot be generated from periodic hexagrids.

B. Duals of icosahedral quasiperiodic hexagrids

For the remainder of this paper we focus on a subset of quasiperiodic hexagrids that plays the same role in three dimensions as the Fibonacci pentagrids in two dimensions—the Fibonacci hexagrids. Our aims are to show that duals of these can be analyzed using techniques similar to those introduced for the 2D case and to determine the PLI class.

A Fibonacci hexagrid is composed of six grids each having planes defined by the equation

$$\mathbf{x} \cdot \mathbf{e}_n = x_{nN} = N + \alpha_n + \frac{1}{\tau}\left\lfloor \frac{N}{\tau} + \beta_n \right\rfloor. \tag{24}$$

It is denoted by $\{\alpha_n, \beta_n\}$. As in the 2D pentagonal case, the Fibonacci hexagrid is also a quasilattice with a minimum separation between grid intersection points.

The first task is to determine the conditions for local

congruence of two Fibonacci hexagrids. As in the 2D case we define locally congruent Fibonacci hexagrids as ones that can be made to coincide exactly out to arbitrarily large distances about any point in either hexagrid.

Theorem 5.2. Two Fibonacci hexagrids, $\{\alpha_n,\beta_n\}$ and $\{\delta_n,\gamma_n\}$, are locally congruent if and only if

$$\Delta\alpha_n \equiv \alpha_n - \delta_n = \mathbf{u}\cdot\mathbf{e}_n + p_n + \frac{1}{\tau}q_n \ ,$$

(25)

$$\Delta\beta_n \equiv \beta_n - \gamma_n = \begin{cases} \mathbf{v}\cdot\mathbf{e}_{\langle 3n\rangle} - q_n + \dfrac{1}{\tau}p_n, & n=0,1,\ldots,4 \\[2mm] -\mathbf{v}\cdot\mathbf{e}_n - q_n + \dfrac{1}{\tau}p_n, & n=5 \end{cases}$$

for some vectors $\mathbf{u}$ and $\mathbf{v}$ and integers p_n and q_n.

The proof of this theorem is essentially the same as that of Theorem 4.2. As in the 2D case, a shift in $\mathbf{u}$ can be interpreted as a translation of the quasilattice and a shift in $\mathbf{v}$ can be interpreted as a rearrangement of the sequence of long and short intervals between grid lines. The duals to two hexagrids that are locally congruent are packings in the same LI class. Packings in a continuum of different LI classes can be obtained by beginning with some choice of $\{\alpha_n,\beta_n\}$ and then considering all possible shifts $\Delta\alpha_n$ and $\Delta\beta_n$ that do not satisfy the above criteria.

We next would like to determine which one of these classes contains packings that have the Penrose properties of Sec. IV A. The strategy, in analogy with the 2D case, is to identify those Fibonacci hexagrids which are locally congruent to their deflations—the 3D icosahedral Ammann quasilattices. (The deflation of a Fibonacci hexagrid is the hexagrid obtained by deflating each of its six component grids according to the deflation rule for a 1D Fibonacci sequence, as shown in Fig. 2.) The duals to the Ammann quasilattices are the 3D analogues of the Penrose tilings and the quasilattice can be obtained directly as a simple decoration of the 3D packing. Theorems 4.3 and 4.4 generalize trivially to three dimensions, so that in order to determine the set of $\{\alpha_n,\beta_n\}$ corresponding to the 3D Ammann quasilattices, it is sufficient to identify one example and then consider all possible local congruence transformations.

A computation quite similar to that found in Appendix D shows that one element of the PLI class has $\alpha_n = 1/\tau$, $\beta_n = -\frac{1}{2}$ for all n. One assumes that an icosahedrally symmetric solution can be found in which $\alpha_n = \alpha$ and $\beta_n = \beta$ for all n, derives conditions on α and β by applying Eqs. (25) to $\alpha - \alpha^*$ and $\beta - \beta^*$, and finds that there exist three solutions corresponding to three distinct packings with complete icosahedral symmetry. Since the presentation of the details would be both tedious and somewhat repetitive, we will simply verify the result here.

From Eqs. (10) and (11) we find that a deflation of $\{\alpha_n = 1/\tau, \beta_n = -\frac{1}{2}\}$ corresponds to

$$\Delta\alpha_n \equiv \alpha_n - \alpha_n^* = \frac{\tau}{2}$$

and

(26)

$$\Delta\beta_n \equiv \beta_n - \beta_n^* = \frac{-1}{2\tau} \ .$$

If $\{\alpha_n = 1/\tau, \beta_n = -\frac{1}{2}\}$ corresponds to an Ammann quasilattice, $\{\alpha_n,\beta_n\}$ must be locally congruent to $\{\alpha_n^*,\beta_n^*\}$; thus, $\Delta\alpha_n \equiv \alpha_n - \alpha_n^*$ and $\Delta\beta_n \equiv \beta_n - \beta_n^*$ must satisfy the constraints of Eqs. (19). The first of these can be satisfied for $\mathbf{u} = (0,0,5\tau/2)$:

$$\frac{\tau}{2} = \frac{5\tau}{2}\left[\frac{1}{\sqrt{5}}\right] + p_n + \frac{1}{\tau}q_n, \quad n=0,1,\ldots,4$$

and

(27)

$$\frac{\tau}{2} = \frac{5\tau}{2} + p_n + \frac{1}{\tau}q_n, \quad n=5 \ .$$

Using $\sqrt{5} = 2\tau - 1$ we find that these can both be satisfied by $p_n = -1$, $q_n = 0$ for $n = 0,1,\ldots,4$ and $p_5 = -2$, $q_5 = -2$. It is a simple matter to check that the second of Eqs. (25) is satisfied by $\mathbf{v} = (0,0,5/2\tau^2)$.

Hexagrids locally congruent to $\{\alpha_n = 1/\tau, \beta_n = -\frac{1}{2}\}$ correspond to other Ammann quasilattices and the set of all hexagrids locally isomorphic to this one constitute the PLI class. From the 2D case, we know that the cell shapes, the deflation rules and a set of matching rules can all be derived from the duals to the Ammann quasilattices. Before this can be done for the 3D case, though, there is one important subtlety to be dealt with: the 3D Ammann quasilattices are *singular* in the extreme; that is, there are many points at which more than three grid planes intersect. In fact, anywhere one might have expected an intersection of three planes whose dual is an oblate rhombohedron, additional planes pass through the intersection making it singular.

C. Singularities revisited

In the 2D pentagonal case, *singular* periodic pentagrids in the PLI class can be resolved by any small shifts in the grids (the γ_n's) which keep $\sum_n \gamma_n$ constant and the duals to the resolved grids are Penrose tilings.[9] Thus, the singular periodic pentagrids in the PLI class can be considered as a degeneracy of two or more PLI class pentagrids. For the 2D case, the Ammann quasilattice whose dual also corresponds to the Penrose tilings is not singular.

In the 3D icosahedral vertex model, the PLI class cannot be generated by duals to periodic hexagrids and the Ammann quasilattice, as we have shown above, must be singular. Any transformation of the $\{\alpha_n,\beta_n\}$ of the form of Eqs. (25) translates the quasilattice and/or rearranges the sequence of long and short intervals in the grid. Such transformations do not resolve the singularities; at most they shift the location of the singularities. *The only transformation of $\{\alpha_n,\beta_n\}$ that resolve the singularities do not correspond to local congruence transformations and, therefore, result in a new Fibonacci pentagrid that is not in the PLI class.*

The fact that PLI class hexagrids are inherently singular suggests that we treat the singularities in a different way than we did for the 2D periodic pentagrids. Rather than resolve the singularities by shifting grids, we introduce a unit-cell shape for each type intersection in the hexagrid, where the type of intersection is characterized by the number of intersecting planes (the *order* of the

singularity). The dual to a nonsingular intersection is a rhombonhedron; in this case, the only nonsingular intersections are duals to prolate rhombohedra. The cell dual to a singular intersection is a zonohedron with vertices given by the points dual to the open regions in grid space that surround the singular intersection. Each zonohedron is actually a polyhedron that can be constructed from the two fundamental rhombohedra. In fact, if we were to resolve the singularity by small shifts in the grids, we would obtain a packing in which each zonohedron is resolved into constituent rhombohedra. It appears that such a resolved structure can be obtained by grid and direct projections. However, it is the zonohedral packing and not the rhombohedral one that possesses all the intriguing Penrose properties. Thus, for the special case of the 3D icosahedral PLI class, it is actually simpler to describe the structure in terms of the zonohedra.

Three zonohedral unit cells arise in addition to the prolate rhombohedron (see Table I for a precise specification of the unit cells), corresponding to the following three types of singularities.

(1) Sixfold: Six planes, one from each grid, meet in a single point. The resulting dual shape is a *rhombic triacontahedron*, a polyhedron with thirty identical rhom-

TABLE I. Specification of unit-cell shapes for the PLI class packing and their deflations. Upper: The vertices of each zonohedron are listed for the orientation in which they appear in Figs. 11(a)—11(d). The edges of the zonohedron are constructed by joining each pair of points that differ by a single e_n. Lower: The vertices of the deflation decoration of each of the zonohedra. The points listed are those which lie at the vertices of the deflated cells [the vertices of the shaded polygons in Figs. 11(a)—11(d)]. The edges of the cells can be constructed by joining all vertices that differ by a single ϕe_n. Note that certain points which are both vertices of an original zonohedron and vertices of a deflated zonohedron appear differently in the two contexts. For example, $\phi\phi\phi00\phi$ in the deflation of the rhombohedron is the same point as 010001 in the original rhombohedron. Notation: $k_0k_1k_2k_3k_4k_5 \equiv \sum_{n=0}^{5} k_n e_n$, where the e_n's are defined by Fig. 8.

Unit cells with edge length 1							
Rhomb	000000	000001	100000	010000	110000	100001	010001	110001
Dodec.	000000	100000	000010	100010	001000	001010	101000	001001
	001011	101001	000011	100001	100011	101011		
Icos.	000000	100000	010000	001000	000100	000010	110000	011000
	001100	000110	100010	001110	100110	110010	111000	011100
	011110	101110	110110	111010	111100	111110		
Triac.	000000	100000	010000	001000	000100	000010	110000	011000
	001100	000110	100010	110010	111000	011100	001110	100110
	110001	011001	001101	000111	100011	110011	111001	011101
	001111	100111	011111	101111	110111	111011	111101	111111

Deflations of above cells $\phi = 1/\tau$, $\bar\phi = -\phi$, $\hat\phi = 2\phi$

Rhomb. — 000000 here corresponds to 000000 in above rhombohedron

000000	φ00000	0φ0000	00000φ	φφ0000	φ0000φ	0φ000φ	φφ000φ
φφφ00φ	φφ0φ̄0φ	φφ00φφ					

Dodec. — 000000 here corresponds to 000010 in above dodecahedron

000000	00φ000	00000φ	00φ00φ	0φ0000	0φ000φ	0φφ000	0φφ00φ
0φ0φ00	0φφφ00	0φ0φ0φ	0φφφ0φ	φφ000φ	0φ00φφ	φφ00φφ	φφφ00φ
0φφ0φφ	φφφ0φφ	φ̄φφ000	0φφ0φ̄0	φ̄φφ0φ̄0	φ̄φφ00φ	0φφ0φφ	φ̄φφ0φ̄φ
0φφφ0φ	0φ̂φ00φ						

Icos. — 000000 here corresponds to ½(111111) in above icosahedron

000000	φ00000	0φ0000	00φ000	000φ00	0000φ0	φ̄00000	0φ̄0000
00φ̄000	000φ̄00	0000φ̄0	00000φ̄	φ̄0000φ̄	0φ̄000φ̄	00φ̄00φ̄	000φ̄0φ̄
0000φ̄φ̄	φ̄φ̄0000	0φ̄φ̄000	00φ̄φ̄00	000φ̄φ̄0	φ̄0000φ̄0	φ̄φ̄0000φ̄	0φ̄φ̄00φ̄
00φ̄φ̄0φ̄	000φ̄φ̄φ̄	00000φ					

Triac. — 000000 here corresponds to ½(111111) in above triacontahedron

000000	φ00000	0φ0000	00φ000	000φ00	0000φ0	00000φ	φ̄00000
0φ̄0000	00φ̄000	000φ̄00	0000φ̄0	00000φ̄	φ0000φ	0φ000φ	00φ00φ
000φ0φ	0000φφ	φ̄0000φ̄	0φ̄000φ̄	00φ̄00φ̄	000φ̄0φ̄	0000φ̄φ̄	φφ0000
0φφ000	00φφ00	000φφ0	φ000φ0	φ̄φ̄0000	0φ̄φ̄000	00φ̄φ̄00	000φ̄φ̄0
φ̄0000φ̄0	φ00φ00	0φ00φ0	φ̄0φ000	0φ̄0φ00	00φ̄0φ0	φ̄00φ00	0φ̄00φ0
φ0φ̄000	0φ0φ̄00	00φ0φ̄0	φφ000φ	0φφ00φ	00φφ0φ	000φφφ	φ000φφ
φφ0φ̄00	0φφ0φ̄0	φ̄0φφ00	0φ̄0φφ0	φ0φ0φ0	φ̄φ̄000φ̄	0φ̄φ00φ̄	00φ̄φ̄0φ̄
000φ̄φ̄φ̄	φ̄000φ̄φ̄	φ̄φ̄0φ00	0φ̄φ̄0φ0	φ0φ̄φ00	0φ0φ̄φ0	φ̄0φ0φ0	

bic faces. Since no direction has been singled out it is clear that the triacontrahedron has the full symmetry of a regular icosahedron or dodecahedron. It can be resolved into ten prolate and ten oblate rhombohedra in many different ways, but in none of them is the full icosahedral symmetry preserved.

(2) Fivefold: The dual to a fivefold singularity is a *rhombic icosahedron*. There are six ways to make a fivefold singularity, each obtained by removing a plane in one of the directions from a sixfold one. The six icosahedra thus obtained are clearly just different rotations of the same shape. The icosahedron has a pentagonal axial symmetry about the direction of the "missing" grid. It can be resolved into five prolate and five oblate rhombohedra.

(3) Fourfold: The dual of a fourfold singularity is a *rhombic dodecahedron*. There are fifteen possible orientations of the dodecahedron, corresponding to the fifteen different ways in which two planes can be removed from a sixfold intersection. (To see that the same shape is always obtained, consider the removal of a single plane from a fivefold intersection. The axial symmetry of the fivefold means that the same configuration is left no matter which plane is removed.) The dodecahedron can be resolved into two prolate and two oblate rhombohedra.

We note that the zonohedral interpretation of singularities could also be used for singular periodic hexagrids, rather than resolving the singularities into rhombohedra by shifting grids.[27] However, singularities can only appear in a trivial way for periodic hexagrids. For example, a periodic hexagrid can have at most one sixfold singularity and all sixfold singular hexagrids are equivalent. (The constraint on the γ_n's necessary for six grid planes to intersect at a single point is sufficient to determine the whole hexagrid, up to a translation.) Furthermore, the density of singular intersections in any hexagrid must be zero because of the incommensurability of the periodic sublattices.

D. The 3D Penrose local isomorphism class

The packings dual to the Fibonacci hexagrids locally isomorphic to $\{\alpha_n = 1/\tau, \beta_n = -\frac{1}{2}\}$ share all of the remarkable properties of the 2D Penrose tilings. A section of a packing in the PLI class is displayed in Fig. 9. The three layers pictured in the figure overlay one another to form a thick slice. The twenty rhombohedra indicated in the figure, for example, actually fit together to form an icosahedrally symmetric star. All twenty of them have a point in common (the center of the star). We note a few characteristics of the structure that are recognizable upon inspection of several such pictures or simple analysis of the PLI class quasilattices.

(i) As noted earlier, there are no oblate rhombohedra in the packings in the PLI class. Four types of unit cell appear; the triacontahedron, the icosahedron, the dodecahedron, and the prolate rhombohedron, with volumes in the ratios $10\tau{:}5\tau{:}2\tau{:}1$.

(ii) There are local clusters of unit cells that have complete icosahedral point symmetry. The most obvious are the triacontahedron itself and the "star" of twenty rhom-

bohedra arranged to form a stellated icosahedron. There are three complete packings with a (single) center of icosahedral point symmetry. One of these has a triacontahedron at its center, the next shell being composed of thirty dodecahedra. The other two have a star at their centers, one having twelve icosahedra as the next shell, the other having twelve triacontrahedra.

(iii) There is a homogeneity about the packings reminiscent of the Penrose tilings. Given any finite region, there are others identical to it relatively close by.

The key to understanding these properties, as well as the matching and deflation rules, is the decoration of the unit cells that produces the 3D Ammann quasilattice generated by grid planes that we will term *Ammann planes*. Because the dual to the Ammann quasilattice is the zonohedral tiling, and because the deflation of the Ammann quasilattice is locally congruent to the original, the Ammann planes represent a simple decoration of the zonohedral unit cells in exactly the same sense that the Am-
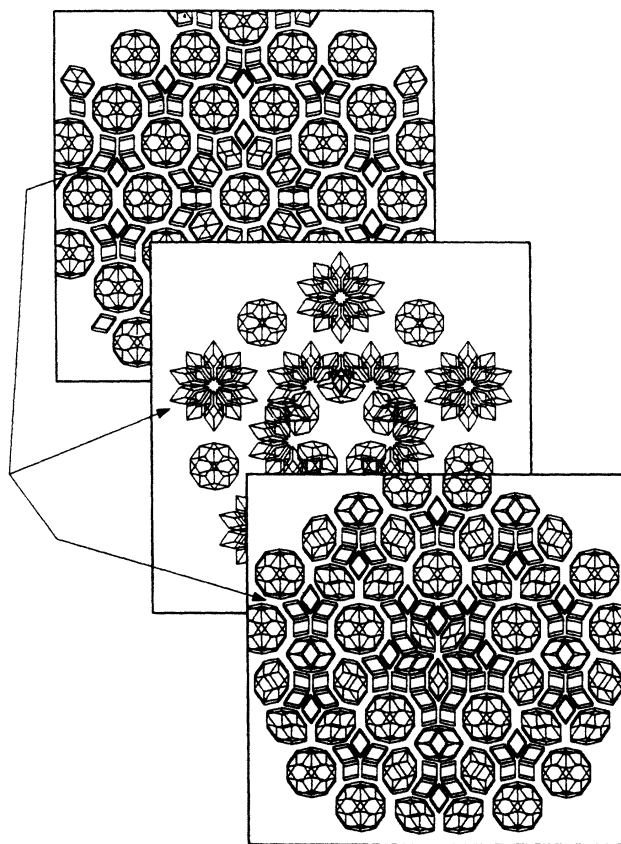

FIG. 9. Thick slice of an icosahedral packing in the PLI class. Three layers of cells are depicted which overlay each other to form the slice. (The unit cells have been drawn as wire frames.) In the 3D packing, a single point is shared by all twenty of the rhombohedra that are indicated by arrows (five in the top frame, ten in the middle, and five in the bottom). The central triacontahedron in the top frame is surrounded by thirty, dodecahedra, ten of which are visible in the top frame, five in the middle, and five in the bottom.

mann lines are a decoration of the 2D Penrose tiles. Just as in the 2D case, the deflation of the 3D zonohedral cells can be determined by taking the dual of the Ammann plane decoration of the cells. A set of matching rules for the zonohedral cells consists of decorating the cells with Ammann planes and then demanding that two cells match face to face if and only if the planes that decorate the cells are continued (along the same plane) across the interface. The detailed method by which we obtained the positions of the planes in the zonohedra and the correct deflation of each cell is difficult to explain without access to some 3D models. We will simply present the results, which can

FIG. 10. Ammann plane decoration of the unit cells of the PLI class packing. A precise specification of the locations of these planes is given in Table II. Parallel planes are shaded the same way. The zonohedra and Ammann planes are shown exactly as they would appear to the eye if the faces of the zonohedra were transparent and the Ammann planes were opaque. In (b), dashed lines indicate edges of the dodecahedron that are seen through transparent faces. A smaller version of each cell is also shown with matching rules and shadings that facilitate comparison with Figs. 11 and 13. (a) The rhombohedron. Its decoration has trigonal symmetry about the long diagonal of the rhombohedron. (b) The dodecahedron. This decoration has two planes of reflection symmetry. One of these reflection planes is nearly perpendicular to the page and contains the long diagonal of the "front" face of the dodecahedron. The other is parallel to the front face and contains the long diagonal of the "top" face (the long edge of the Ammann plane shaded with a square grid). Note that the dodecahedron itself has a third mirror plane, but this symmetry is not respected by the Ammann plane decoration. (c) The icosahedron. This decoration has pentagonal symmetry about the axis of the icosahedron. On the side which is hidden from view is another plane (parallel to the one shaded with double lines) which is intersected by planes forming a star exactly like those found on each plane decorating the triacontahedron in (d). (d) The triacontahedron. The planes of this decoration join to form a perfect great icosahedron.

TABLE II. Specification of the Ammann plane decoration of the unit cells of the PLI class packing. Each Ammann plane that passes through a given cell intersects at least two vertices of that cell. Each Ammann plane is specified by the e_n that is orthogonal to the plane and a list of the unit cell vertices that the plane intersects. When two parallel Ammann planes (i.e., associated with the same e_n) pass through the same cell a set of unit cell vertices is shown on two separate lines for each plane and the spacing between them (L or S) is noted. The orientation of each cell with respect to the e_n's is the same as in Figs. 11(a)—11(d).

Shape	Normal	Points in plane[a]					Spacing
Rhomb.	e_5	100000	010000				
	e_0	010000	000001				
	e_1	100000	000001				
	e_2	110001	010000	000001			
	e_3	110001	100000	010000			
	e_4	110001	100000	000001			
Dodec.	e_5	100010	001010	101000			
	e_0	000000	001010	001001			L
		100010	100001	101011			
	e_1	000000	001010	000011	100010		S
		001001	101011	101000	100001		
	e_2	000000	100001	000011			
	e_3	001001	101011	001010	000011		S
		000000	100010	100001	101000		
	e_4	000000	101000	001001			L
		100010	000011	101011			
Icos.	e_5	110000	011000	001100	000110	100010	S
		111100	111010	110110	101110	011110	
	e_0	110000	100010	110110	111010		L
		000000	011000	000110	011110		
	e_1	110000	011000	111010	111100		L
		000000	001100	100010	101110		
	e_2	011000	001100	111100	011110		L
		000000	000110	110000	110110		
	e_3	001100	000110	011110	101110		L
		000000	100010	011000	111010		
	e_4	000110	100010	101110	110110		L
		000000	110000	001100	111100		
Triac.[b]	e_5	110000	011000	001100	000110	100010	L
		111001	011101	001111	100111	110011	

[a] Notation: $k_0 k_1 k_2 k_3 k_4 k_5 \equiv \sum_{n=0}^{5} k_n e_n$, where the e_n's are defined by Fig. 8.

[b] Plus an equivalent pair of planes in each of the other five directions.

then be checked by overlaying an Ammann quasilattice and its dual. The conceptual problem is the determination of the $\{\alpha_n, \beta_n\}$ for the PLI class, which has already been solved analytically.

The Ammann plane decoration of the four cells is illustrated in Figs. 10(a)—10(d) and a precise definition of each plane is given in Table II. Each line of Table II corresponds to a different plane in the decoration. We have listed all of the zonohedron's vertices through which the plane passes and the e_n normal to the plane. The vertices of the zonohedra are specified (as in Table I) by coefficients of the e_n's. When two parellel planes from the same grid pass through a single zonohedron they are listed as a pair and the spacing between them noted. Only one

orientation of each zonohedron is explicitly described since the same decoration applies to all unit cells of the same shape, i.e., the Ammann planes constitute a simple decoration.

All of the singular intersections in the Ammann plane quasilattice occur at vertices of unit cells and all the intersections dual to rhombohedra (nonsingular intersections of three planes) occur in the interiors of cells. The spacings between parallel planes are, of course, either L or S, where $L:S = \tau:1$. For example, the center of the triacontahedron lies at the midpoint of an L spacing between each of the six grids and the center of the icosahedron lies in an S spacing along its axial direction. The order of the singularities for Ammann plane intersections at the vertex

of a unit cell depends, in principle, on the cells that adjoin it since their decorations can add other intersection planes at the vertex and increase the order of the singularity. In most cases, though, the order of the singularities at the cell vertices can be determined from the allowed sequences of L and S spacings between planes in the various grids. For instance, in the Ammann plane decoration of the prolate rhombohedron, three planes intersect one of the "acute" vertices; see the lower corner in Fig. 10(a). (An acute vertex is one which lies at the intersection of three edges, any pair of which intersect at an acute angle.) Although one may have thought that the order of the

singularity at the vertex depends upon the position and orientation of the Ammann planes in unit cells which adjoin the rhombohedron, a closer examination of the rhombohedral decoration shows that the acute vertex must always correspond to a sixfold singularity: There is a nonsingular intersection of three planes along the diagonal connecting this first acute vertex to the second [at the uppermost corner of Fig. 10(a)]. The spacing from the planes to the vertex is L. Since there is no plane parallel to these that lies in between at spacing S (which would cut through the rhombohedron), there must be planes parallel to these which lie at spacing L and intersect the rhom-

FIG. 11. Deflation decoration of the unit cells of the PLI class packing. Each cell is divided into pieces (labeled A—G) which are shown in exploded views. The faces of the pieces which become faces of the deflated cells are shaded. The unshaded faces adjoin other pieces and lie in the interior of the deflated cells. We have attempted to label enough pieces so that all of them can be identified without cluttering the picture with too many arrows. The precise locations of the vertices of the decoration are given in Table I. The star of vectors in each figure indicates the orientation of each cell as it is described in the table. (a) The rhombohedron deflates to one A, three B's, and one C. (b) The dodecahedron deflates to four A's, two B's, four D's, and two E's. (c) The icosahedron deflates to ten A's, five D's, five F's, and one G. (d) The triacontahedron deflates to twenty A's and twelve G's.

bohedron just at the vertex. Thus, the vertex lies at the intersection of the three planes explicitly shown in the rhombohedral decoration plus three which are forced to occur but which appear explicitly only in adjoining unit cells. An obvious consequence is that the allowed configurations of adjoining unit cells is rather constrained.

The deflation of each unit cell can be determined from the duals to the Ammann planes. Table I gives the exact positions of the vertices of the deflation decoration and this decoration is depicted in Fig. 11. The deflation divides each cell into *pieces* which can rejoin to form the four cell shapes in a deflated packing. In the figure, the subdivision of a cell into the *pieces* is shown in an exploded view. Figure 12 shows how the pieces can rejoin to form new (deflated) unit cells. (Only one way to form the triacontahedron from the pieces is shown even though, in general, triacontahedra are formed from several different combinations of pieces C, E, F, and G in a deflated packing.) A subtlety is that some pieces serve double roles. These pieces are associated with Ammann plane intersections at the vertices of a cell for which the order of the singularity and the dual cell shape depend on the adjoining unit cells. One of them, B, is sometimes part of a deflated dodecahedron and sometimes part of an icosahedron. Another, G, participates in both deflated triacontahedra and icosahedra. This makes it more difficult to implement the deflation procedure than it is in the 2D case, but the appropriate identity of these pieces is always determined by an adjoining cell.

Note that the Ammann plane decoration of the unit cells does not always have the same symmetry as the unit cells themselves. For example, the rhombohedron itself is symmetric end to end, but the Ammann plane decoration distinguishes one end from the other (see Fig. 10). The deflation (and matching rule decorations to be discussed below) have this same property, just as in the 2D Penrose tiling. Thus, to implement repeated deflations, it is necessary to specify both the shape and orientation of the deflated cells. Decorating the cells with either the Ammann planes or matching rules automatically keeps track of the orientation (e.g., which end of a deflated rhombohedron is which), because all these decorations have the same symmetry. The orientations of the deflated cells are determined by the deflation of the Ammann quasilattice that decorates the original cells. This represents a unique,

FIG. 12. The way in which the pieces of Figs. 11(a)—11(d) join to form the deflated cells. The deflated rhombohedron is not shown because it is formed by a single piece A. Only one of several possible ways to make the triacontrahedron is depicted. The others involve various combinations of pieces C, E, F, and G.

deterministic deflation prescription. In terms of Figs. 11 and 12, this prescription corresponds to the following. (1) The triacontahedron poses no problems because all of its possible orientations are equivalent. (2) Given the orientation of the pieces which rejoin to form a once-deflated dodecahedron or icosahedron, the orientation of the *next* deflation decoration of each can be defined. In Fig. 12 the deflated dodecahedron is shown in the orientation that allows it to be *next* deflated as shown in Fig. 11. The deflated icosahedron of Fig. 12 is further deflated by identifying the vertex shared by the five B pieces with the vertex shared by the five D's in the deflation decoration of Fig. 11. (3) The rhombohedron is a bit more complicated. Let us define the direction of a rhombohedron to be along the diagonal connecting the two acute vertices and pointing in the direction of the acute vertex that lies at the intersection of three Ammann planes in the rhombohedral Ammann plane decoration. The direction of the undeflated rhombohedron is towards the upper right hand corner (along $e_5 + e_1 + e_0$) in Fig. 11. The deflated rhombohedra in Fig. 11 then are all directed outwards from the interior of the undeflated zonohedral unit cell.

Given these deflation rules, it is possible to obtain an arbitrarily large packing from repeated deflation of a finite cluster of unit cells.

Although some pieces (B and G) in the deflation decoration serve double roles in forming new unit cells, the deflation rules as specified in Table I and Fig. 11 can be used to derive the relative numbers of rhombohedral (r), dodecahedral (d), icosahedral (i), and triacontahedral (t) unit cells in the packing:

$$r:d:i:t = 1:\frac{3-\tau}{6\tau+2}:\frac{\tau-1}{3\tau+1}:\frac{1}{6\tau+2}$$

$$\approx 1:0.118:0.106:0.085 . \tag{28}$$

This computation is left as a challenging exercise for the interested reader. These analytical results agree with brute force numerical counts.

Finally, as stated earlier, matching rules can be formulated for the cells such that the only space-filling packings possible consistent with the rules correspond to packings in the PLI class. One form of the matching rules is afforded by the Ammann planes themselves. If adjacent cells are required to be placed so that their Ammann plane decorations join to form continuous planes, the result must be a packing in the PLI class. It is clear that no periodic structures can be produced by such a matching rule because the Ammann planes in each cell are forced into an icosahedral grid pattern in which there is a minimum separation between grid intersections—an icosahedral quasilattice. That the quasilattice is necessarily an Ammann quasilattice can be inferred from the correspondence between the Ammann plane decoration, the matching rules and the deflation rules.

Other realizations of these same matching rules can be generated noting that the Ammann planes distinguish only three different types of rhombic faces on surfaces of the unit cells. Any marking on the faces that distinguishes them and their orientation in the same way as the Ammann planes is an equivalent matching rule. We simply stipulate that two adjacent cells must be joined along
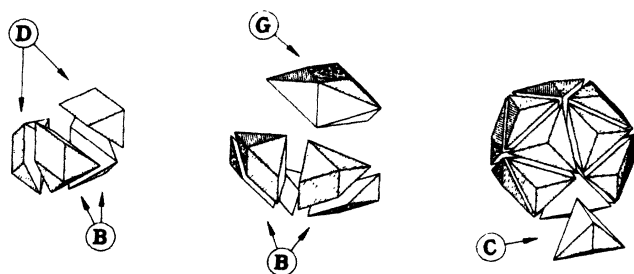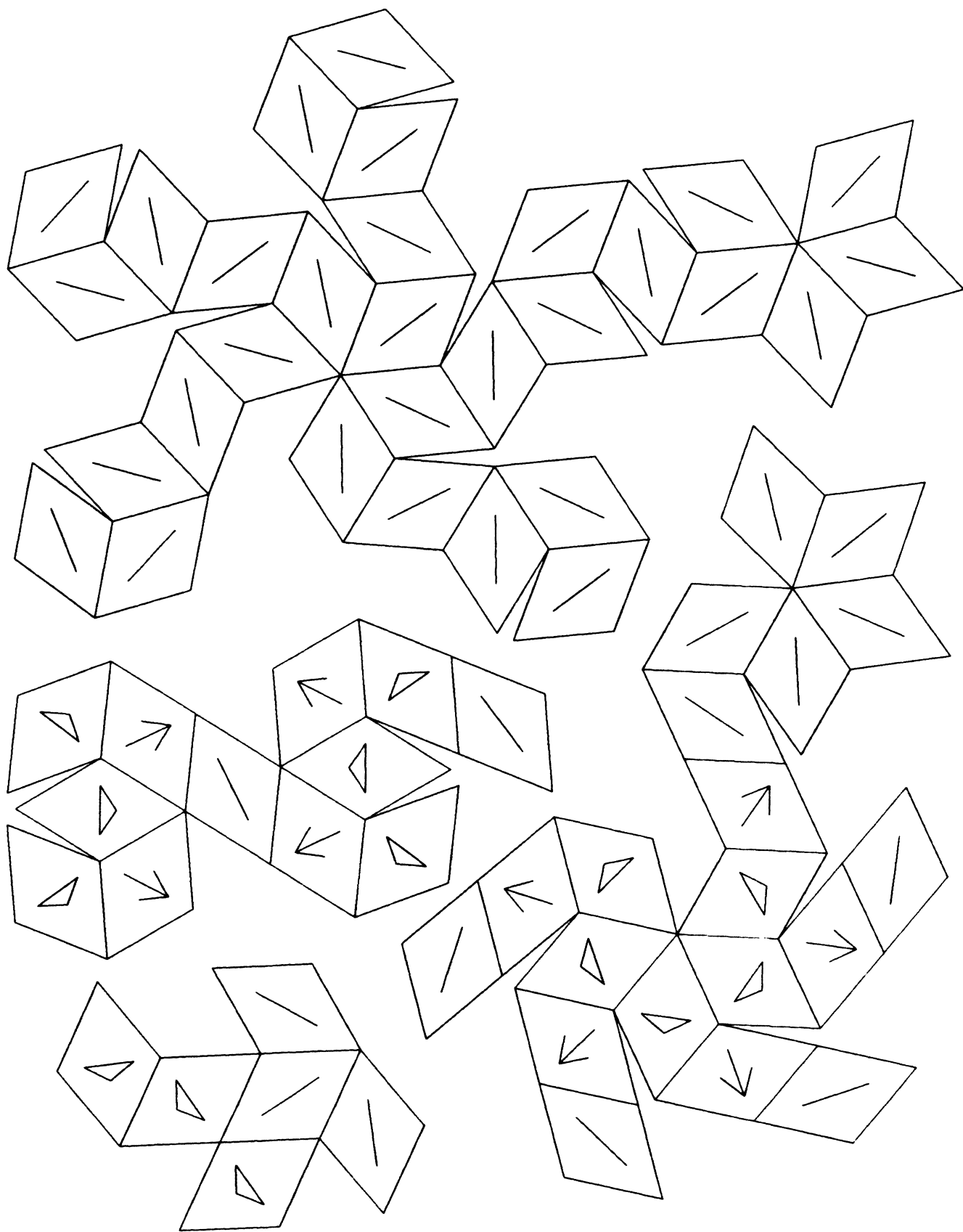
FIG. 13. Matching rule decoration for the unit cells of the PLI class packing. The cells can be constructed by cutting, folding, and taping. (Which edges get taped together becomes obvious as the procedure is carried out.) The matching rule that forces a PLI class packing is simply that adjacent cells are required to join along identical faces with the same orientation.

faces with identical markings and orientations. In Fig. 13 we illustrate such a decoration. The zonohedra have been cut along certain edges so that they could be flattened out. They can be reconstructed by cutting, folding, and taping. Note that two faces marked with triangles or arrows can only match one way but two faces marked with the line segment can match two ways.

The Ammann plane decorations of the zonohedra can also be viewed as a decoration of the oblate and prolate rhombohedra that can adjoin to form them. In this case, the expression of the matching and deflation rules is rather complicated since the Ammann planes correspond to context dependent decorations of the rhombohedra. That is, two prolate rhombohedra, say, can be decorated in different ways by the Ammann planes and so have different rules associated with them. Such context dependent rules are difficult to state concisely—the "simple" rules for the zonohedra are difficult enough to express. Although the rhombohedral unit cells are the most useful for describing the general 3D icosahedral quasicrystal packing, the zonohedra are the easiest for describing the PLI class tilings. As unfortunate as this may be, it must be accepted as one of the necessary subtleties of the 3D icosahedral construction.

VI. CONCLUSIONS

Two quasicrystals packings with the same orientational symmetry, quasiperiodicity and unit-cell shapes may nevertheless correspond to very different arrangements of the unit cells. The different arrangements can be grouped into equivalence classes we have termed local isomorphism (LI) classes. Different methods of constructing quasicrystal packings—grid projections, direct projections, matching and deflation rules, and the GDM—do not generate the same spectrum of LI classes. The GDM packings, though, encompass all those generated by the other methods (as conventionally defined in the literature) plus an infinitely greater set.

The Venn diagram in Fig. 14(a) illustrates what we know thus far about possible quasilattice packings for the 3D icosahedral (vertex) model. The most general class of

icosahedral packings is obtained via GDM using an arbitrary icosahedral 6-grid. The subset that is the simplest to analyze consists of packings generated from planar hexagrids with a periodic or quasiperiodic sequence of spacings between the grid planes. In this paper, the largest set of packings we have analyzed is the one generated by a special choice of quasiperiodic hexagrids—Fibonacci hexagrids—for which there is a Fibonacci sequence of long and short spacings between grid planes. The duals to Fibonacci hexagrids include a spectrum of different LI classes which can be parametrized by $\{\alpha_n,\beta_n\}$ (see Sec. V). The set of 3D packings analogous to the Penrose tiling are also indicated in Fig. 14(a) and form the Penrose local isomorphism (PLI) class. This class is the one which can be generated by matching and deflation rules and corresponds to a *single* LI class. This class can also be generated by the GDM using a special choice of Fibonacci hexagrids corresponding to Ammann quasilattices. Direct projections and grid projections from a 6D hypercubic lattice, as well as GDM for a periodic hexagrid, all yield the same *single* LI class of packings which is not the PLI class and which, as far as we know, has no distinctive properties. We have indicated this set with a dotted boundary because we conjecture that this LI class can also be obtained as duals to Fibonacci hexagrids, but we have not proven it. In Fig. 14(b), we show the Venn diagram appropriate to the 2D pentagonal quasicrystals. The only difference in this case is that the projection techniques generate a set of tilings in an infinite number of distinct LI classes, including the PLI class. We have indicated the set by a dotted line in this case because, although we have shown that the PLI class can also be generated via the GDM for Fibonacci pentagrids, we do not know about the other LI classes. (We conjecture that some but not all of these can be generated from Fibonacci pentagrids.)

Understanding and distinguishing LI classes has physical significance, as we argued in paper I. Two packings in different LI classes have different diffraction peak intensities and free energies. They should not be regarded as degenerate states for the purpose of computing the ground-state degeneracy. Also, determining the atomic decorations of unit cells from diffraction peak intensities is much more difficult for quasicrystals than crystals since modulations in intensity between two samples may be due to variation in atomic decoration *or* LI class.

We have introduced a formalism that allows us to classify quasicrystal packings at least for those cases generated by the GDM for periodic and Fibonacci N-grids. The method can be extended for other quasiperiodic N-grids where the quasiperiodicity is given by Eq. (3). However, a general formalism that includes all possible packings does not yet exist.

We have used the formalism to find the special PLI class of quasicrystal packings for the 2D pentagonal and 3D icosahedral case. We note here that the method has been fully extended for the 2D octagonal case as well as found to work in all its details.[13] We have made some progress in the case of 2D sevenfold and twelvefold symmetry, but we do not yet have a complete construction of the PLI class for these or any other symmetries. Clearly, there are a number of open mathematical and, potentially,
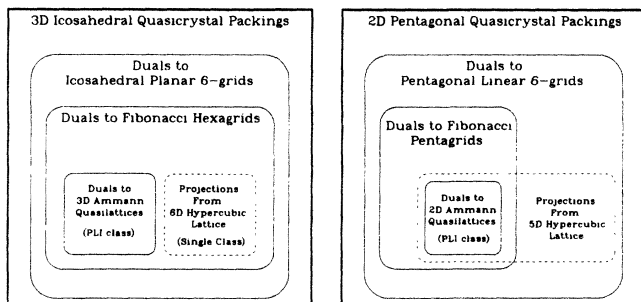

FIG. 14. Venn diagrams summarizing our understanding of various sets of packings and tilings discussed in the text. The dashed lines emphasize our incomplete understanding of the set of packings obtainable by projection from hypercubic 6D and 5D lattices. We have indicated our best guess in each case.

physical issues that must be resolved for more general symmetries.

The PLI packings may have direct physical significance if the simple matching rules associated with them have physical manifestations through the interactions of atoms or atomic clusters, although we have no reason to suggest that this is the case of I-Al-Mn or related alloys. At the very least, the PLI packings are useful because we have the most number of tools—matching rules, deflation rules, and Ammann quasilattice decorations—with which to analyze them. For example, although there exists a hydrodynamic description of quasicrystal dislocations in terms of density waves,[28] a description in terms of packings of unit cells has not been given previously. We have found that the hydrodynamic description, expressed in terms of spatially varying phases of the density waves, can be translated to describe dislocations in quasilattices, expressed in terms of spatially varying $\{\alpha_n, \beta_n\}$. Far from the dislocation core, a structure should appear (nearly) perfect; for quasilattices this means that regions far from the dislocation core should be locally congruent to the undefected lattice. Finally, to obtain a description of the dislocated structure in terms of a packing of unit cells, we use the fact that, for the particular case of the PLI class, the unit cells can be obtained as a decoration of the Ammann quasilattice. By decorating local configurations of
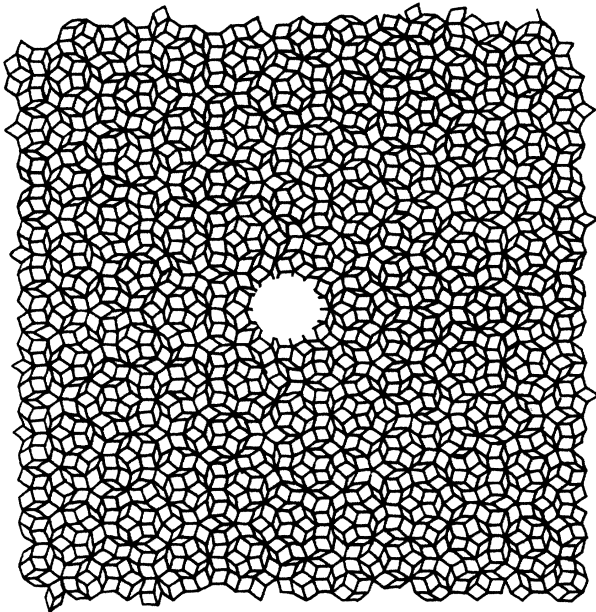

FIG. 15. Portion of a 2D Penrose tiling containing a single dislocation. See Ref. 29 for details of the construction. The dislocation core (represented by the white disk) cannot be filled with tiles. The tiles are all slightly distorted as a result of the dislocation, the amount of distortion decreasing with increasing distance from the core. A construction of the skeleton curves for the dislocated tiling illustrates that extra "half-curves" are added along two independent directions. Although most of the tiles are arranged according to the Penrose matching rules, there are occasionally (even far from the core) local configurations that violate the rules. The description in terms of unit cells corresponds with the hydrodynamic description of dislocations given in Ref. 27.

vertices in the dislocated Ammann quasilattice in the same way (allowing for small distortions in the rhombic shapes), we are able to construct the dislocated unit-cell packing for the PLI class. Figure 15 has been produced by first generating a dislocated Ammann quasilattice on a computer and then decorating the quasilattice by hand. The detailed construction of the dislocated packing will be described in a later paper.[29]

ACKNOWLEDGMENTS

APPENDIX A: PROOF OF THEOREM 4.1

(i) Proof that $\sum \gamma_n - \sum \gamma'_n = m \Rightarrow \{\gamma_n\}$ is locally isomorphic to $\{\gamma'_n\}$: We first note that if any γ_n or γ'_n is changed by an integer the grid specified by it is unaltered; its lines are merely re-indexed. We can therefore redefine the γ_n's in such a way as to make $m = 0$. Next note that once the line with index $N = 0$ is chosen for each of the grids, the quantity $\sum \gamma_n$ is unaffected by the choice of origin from which the γ_n's are measured. (If the origin is translated by a vector z the change in γ_n is given by $\Delta\gamma_n = z \cdot e_n$. But $\sum_{n=0}^{4} z \cdot e_n = z \cdot \sum_{n=0}^{4} e_n = 0$.)

Now the entire pentagrid is completely determined once the positions of a single line in each grid are specified. Suppose the positions of the $N = 0$ lines in $\{\gamma_n\}$ are all specified and that $\sum \gamma_n = c$. We will show that for any ϵ a choice of origin can be made for $\{\gamma'_n\}$ (which is equivalent to a translation by some z) that makes $\gamma'_n - \gamma_n < \epsilon \forall n$.

Considered alone, the two grids having directions e_2 and e_2 form a periodic lattice of rhombuses with short diagonals oriented in the x direction. In units of the grid spacing the length of the short diagonal is $2/\tau$ and the length of the long one is $2/\sqrt{3} - \tau$. Similarly, the grids associated with e_1 and e_4 form a periodic lattice of rhombuses with diagonals of length 2τ in the x direction and

$2/\sqrt{2+\tau}$ in the y direction. These two lattices are clearly incommensurate with each other in both the x and y directions. [Note that $\sqrt{2+\tau}/\sqrt{3-\tau}=\tau$.] Given any vector $\mathbf{v}$ we can therefore find a pair of points $\mathbf{P}_{23}$ and $\mathbf{P}_{14}$, one on each lattice, such that $|\mathbf{P}_{23}-\mathbf{P}_{14}-\mathbf{v}|<\epsilon/2$.

Let $\mathbf{v}$ be the displacement from the intersection point of the $N=0$ lines of grids 2 and 3 to the intersection point of the $N=0$ lines of grids 1 and 4 in $\{\gamma_n\}$. We can now locate $\mathbf{P}_{23}$ and $\mathbf{P}_{14}$ in $\{\gamma'_n\}$, designate the lines which intersect at these points as $N=0$ lines, and choose the origin such that $\gamma'_1=\gamma_1$ and $\gamma'_4=\gamma_4$. Because $|\mathbf{P}_{23}-\mathbf{P}_{14}-\mathbf{v}|<\epsilon/2$ we have $|\gamma'_2-\gamma_2|<\epsilon/2$ and $|\gamma'_3-\gamma_3|<\epsilon/2$. Finally, we note that γ_0 and γ'_0 are fixed by the condition $\sum\gamma_n=\sum\gamma'_n=c$ which implies $|\gamma'_0-\gamma_0|<\epsilon$.

Since γ'_n can be made arbitrarily close to γ_n for all n and for any choice of origin in $\{\gamma_n\}$, the pattern of intersections around the origins of the two pentagrids can be made to agree out to arbitrarily large distances. The two pentagrids therefore yield tilings that coincide exactly in an arbitrarily large region about the vertex dual to the open region containing the origin.

(ii) Proof that $\sum\gamma_n-\sum\gamma'_n\neq m\Rightarrow\{\gamma_n\}$ is not locally isomorphic to $\{\gamma'_n\}$: It is clear that $\gamma'_n-\gamma_n$ cannot be made arbitrarily small for all n simultaneously as this would imply $\sum\gamma'_n-\sum\gamma_n$ could be made arbitrarily small. Since the intersections in a periodic pentagrid run arbitrarily close together it is equally clear that in order for $\{\gamma_n\}$ and $\{\gamma'_n\}$ to be topologically equivalent one must be able to make γ'_n and γ_n arbitrarily close for all n.

In the case of periodic pentagrids it is easy to determine the criteria that apply when we expand the definition of local isomorphism to include tilings related by inversions, as in paper I. The pentagrid (and, therefore, its dual) can be inverted simply by taking $\gamma_n\rightarrow-\gamma_n$. Then, a more general definition of LI class that includes inversions is: $\{\gamma_n\}$ and $\{\gamma'_n\}$ are in the same LI class if and only if[30]

$$\left|\mathrm{mod}_1\sum\gamma_n-\tfrac{1}{2}\right|=\left|\mathrm{mod}_1\sum\gamma'_n-\tfrac{1}{2}\right|.$$

APPENDIX B: PROOF THAT A β TRANSLATION IS EQUIVALENT TO AN UMKLAPP FOLLOWED BY A TRANSLATION

Let $\{\alpha_n,\beta_n\}$ and $\{\delta_n,\gamma_n\}$ be related by a β translation, i.e., $\Delta\alpha_n=0$ and $\Delta\beta_n=\mathbf{z}\cdot\mathbf{e}_{\langle 3n\rangle}$, where $\mathbf{z}$ is of the form

$$\left[\frac{m_1+m_2/\tau}{\cos(2\pi/5)},\frac{m_3+m_4/\tau}{\sin(2\pi/5)}\right].$$

We want to show that these $\Delta\beta$'s can be umklapped over to the $\Delta\alpha$'s and that the resulting $\Delta\alpha$'s are of the form $\mathbf{u}\cdot\mathbf{e}_n$.

Using

$$\cos(2\pi/5)=\frac{1}{2\tau},\quad\cos(4\pi/5)=-\frac{\tau}{2},$$

$$\sin(4\pi/5)/\sin(2\pi/5)=\tau,$$

and the relation $1+\tau=\tau^2$, we find

$$\Delta\beta_0=2m_1+2m_2+\frac{1}{\tau}2m_1,$$

$$\Delta\beta_1=-2m_1-m_2-m_4+\frac{1}{\tau}(-m_1-m_2-m_3+m_4),$$

$$\Delta\beta_2=m_1+m_3+\frac{1}{\tau}(m_2+m_4),\tag{B1}$$

$$\Delta\beta_3=m_1-m_3+\frac{1}{\tau}(m_2-m_4),$$

$$\Delta\beta_4=-2m_1-m_2+m_4+\frac{1}{\tau}(-m_1-m_2+m_3-m_4).$$

These can obviously be umklapped to zero (since each $\Delta\beta_n$ is of the form $p+q/\tau$, where p and q are integers) with the result

$$\Delta\alpha_0=-2m_1+\frac{1}{\tau}(2m_1+2m_2),$$

$$\Delta\alpha_1=m_1+m_2+m_3-m_4+\frac{1}{\tau}(-2m_1-m_2-m_4),$$

$$\Delta\alpha_2=-m_2-m_4+\frac{1}{\tau}(m_1+m_3),\tag{B2}$$

$$\Delta\alpha_3=-m_2+m_4+\frac{1}{\tau}(m_1-m_3),$$

$$\Delta\alpha_4=m_1+m_2-m_3+m_4+\frac{1}{\tau}(-2m_1-m_2+m_4).$$

It is now straightforward to verify that $\Delta\alpha_n=\mathbf{u}\cdot\mathbf{e}_n$, where

$$\mathbf{u}=\left[\frac{-m_2+m_1/\tau}{\cos(4\pi/5)},\frac{-m_4+m_3/\tau}{\sin(4\pi/5)}\right]\tag{B3}$$

which makes it clear that an appropriate translation brings all the $\Delta\alpha_n$'s to zero simultaneously.

We note that the form of a β translation is unique. The steps of the proof can be reversed to show that this form of the $\Delta\beta_n$'s is the only one that, when umklapped to zero, yields a pure translation.

APPENDIX C: PROOFS OF THEOREMS 4.3 AND 4.4

For Theorem 4.3 let $\Delta\alpha_n=\alpha_n-\alpha_n^*$, $\Delta\beta_n=\beta_n-\beta_n^*$, $\Delta\alpha'_n=\alpha'_n-\alpha_n^{**}$, and $\Delta\beta'_n=\beta_n^*-\beta_n^{**}$. We want to show that if there exist $\mathbf{u},\mathbf{v},p_n,q_n$ such that

$$\Delta\alpha_n=\mathbf{u}\cdot\mathbf{e}_n+p_n+\frac{1}{\tau}q_n$$

and

$$\Delta\beta_n=\mathbf{v}\cdot\mathbf{e}_{\langle 3n\rangle}-q_n+\frac{1}{\tau}p_n,\tag{C1}$$

then there must exist $\mathbf{u}',\mathbf{v}',p'_n,q'_n$ such that

$$\Delta\alpha'_n=\mathbf{u}'\cdot\mathbf{e}_n+p'_n+\frac{1}{\tau}q'_n$$

and

$$\Delta\beta'_n=\mathbf{v}'\cdot\mathbf{e}_{\langle 3n\rangle}-q'_n+\frac{1}{\tau}p'_n.\tag{C2}$$

To do this we simply express $\Delta\alpha'_n$ and $\Delta\beta'_n$ in terms of $\Delta\alpha_n$ and $\Delta\beta_n$. Using Eq. (11) (Sec. III B 1) we find

$$\Delta\beta'_n = \tau\beta^*_n - \frac{1}{\tau}\lfloor\beta^*_n\rfloor$$

$$= \tau\beta_n - \tau\Delta\beta_n - \frac{1}{\tau}\lfloor\beta^*_n\rfloor . \tag{C3}$$

But, also from Eq. (11), we have $\tau\beta_n = \Delta\beta_n + \tau^{-1}\lfloor\beta_n\rfloor$. Thus,

$$\Delta\beta'_n = -\frac{1}{\tau}\Delta\beta_n + \frac{1}{\tau}(\lfloor\beta_n\rfloor - \lfloor\beta^*_n\rfloor) . \tag{C4}$$

Similarly, we can use Eq. (10) twice to get

$$\Delta\alpha'_n = -\frac{1}{\tau}\alpha^*_n + \frac{\tau}{2} - \lfloor\beta^*_n\rfloor + \frac{1}{\tau}\lfloor\beta^{**}_n\rfloor$$

$$= \tau\Delta\alpha_n + \lfloor\beta_n\rfloor - \frac{1}{\tau}\lfloor\beta^*_n\rfloor - \lfloor\beta^*_n\rfloor + \frac{1}{\tau}\lfloor\beta^{**}_n\rfloor . \tag{C5}$$

We now note that $\lfloor\beta^*_n\rfloor = \lfloor\beta^{**}_n\rfloor = -1$ because $\lfloor\tau^{-1}(\lfloor x\rfloor - x)\rfloor = -1$ for any $x \notin \mathbf{Z}$ and both are of this form according to Eq. (11). Thus we have

$$\Delta\beta'_n = -\frac{1}{\tau}\Delta\beta_n + \frac{1}{\tau}(1 + \lfloor\beta_n\rfloor) ,$$

$$\Delta\alpha'_n = \tau\Delta\alpha_n + 1 + \lfloor\beta_n\rfloor , \tag{C6}$$

and Eq. (33) is explicitly verified using $\mathbf{u}' = \tau\mathbf{u}$, $\mathbf{v} = -(1/\tau)\mathbf{v}$, $p'_n = p_n + q_n + 1 + \lfloor\beta_n\rfloor$, and $q'_n = p_n$.
For Theorem 4.4 let

$$\Delta\alpha_n = \alpha_n - \alpha^*_n, \quad \Delta\beta_n = \beta_n - \beta^*_n ,$$

$$\Delta\delta_n = \delta_n - \delta^*_n, \quad \Delta\gamma_n = \gamma_n - \gamma^*_n , \tag{C7}$$

$$\Delta A_n = \alpha_n - \delta_n, \quad \Delta B_n = \beta_n - \gamma_n .$$

We want to show that if there exist $\mathbf{u}, \mathbf{v}, p_n, q_n, \mathbf{u}', \mathbf{v}', p'_n, q'_n$ such that

$$\Delta\alpha_n = \mathbf{u}\cdot\mathbf{e}_n + p_n + \frac{1}{\tau}q_n ,$$

$$\Delta\beta_n = \mathbf{v}\cdot\mathbf{e}_{\langle 3n\rangle} - q_n + \frac{1}{\tau}p_n ,$$

$$\Delta\delta_n = \mathbf{u}'\cdot\mathbf{e}_n + p'_n + \frac{1}{\tau}q'_n , \tag{C8}$$

$$\Delta\gamma_n = \mathbf{v}'\cdot\mathbf{e}_{\langle 3n\rangle} - q'_n + \frac{1}{\tau}p'_n ,$$

then there must exist $\mathbf{s}, \mathbf{t}, P_n, Q_n$ such that

$$\Delta A_n = \mathbf{s}\cdot\mathbf{e}_n + P_n + \frac{1}{\tau}Q_n ,$$

$$\Delta B_n = \mathbf{t}\cdot\mathbf{e}_{\langle 3n\rangle} - Q_n + \frac{1}{\tau}P_n . \tag{C9}$$

To do this we want to express ΔA_n and ΔB_n in terms of $\Delta\alpha_n$, $\Delta\beta_n$, $\Delta\delta_n$, and $\Delta\gamma_n$. As we did in the previous proof, we use

$$\frac{1}{\tau}\alpha_n = -\Delta\alpha_n + \frac{\tau}{2} - \lfloor\beta_n\rfloor + \frac{1}{\tau}\lfloor\beta^*_n\rfloor ,$$

$$\tau\beta_n = \Delta\beta_n + \frac{1}{\tau}\lfloor\beta_n\rfloor, \quad \lfloor\beta^*_n\rfloor = -1$$

and similar expressions for δ_n and $\{\gamma_n\}$ to get

$$\Delta A_n = \tau(\Delta\delta_n - \Delta\alpha_n) + \tau(\lfloor\gamma_n\rfloor - \lfloor\beta_n\rfloor) ,$$

$$\Delta B_n = \frac{1}{\tau}(\Delta\beta_n - \Delta\gamma_n) - \frac{1}{\tau^2}(\lfloor\gamma_n\rfloor - \lfloor\beta_n\rfloor) . \tag{C10}$$

The theorem can now be explicitly verified using

$$\mathbf{s} = \tau(\mathbf{u}' - \mathbf{u}) ,$$

$$\mathbf{t} = \frac{1}{\tau}(\mathbf{v} - \mathbf{v}') ,$$

$$P_n = p'_n - p_n + q'_n - q_n + \lfloor\gamma_n\rfloor - \lfloor\beta_n\rfloor , \tag{C11}$$

and

$$Q_n = p'_n - p_n + \lfloor\gamma_n\rfloor - \lfloor\beta_n\rfloor .$$

APPENDIX D: ISOLATION OF THE AMMANN QUASILATTICES

Our aim here is to derive a set of values of α_n and β_n (for the 2D case) whose deflation is locally congruent to the original. We begin by assuming that a symmetric set is possible, i.e., that at least one such set is of the form $\alpha_n = \alpha$, $\beta_n = \beta$ for all n. (If the assumption is incorrect, we should encounter a contradiction.) This obviously implies $\Delta\alpha_n \equiv \alpha_n - \alpha^*_n = \Delta\alpha$, $\Delta\beta_n \equiv \beta_n - \beta^*_n = \Delta\beta$ for all n. We can sum over n in Eqs. (19) (Sec. IV C) then to get a necessary condition on $\Delta\alpha$ and $\Delta\beta$:

$$\sum_n \Delta\alpha_n = P + \frac{1}{\tau}Q ,$$

$$\sum_n \Delta\beta_n = -Q + \frac{1}{\tau}P , \tag{D1}$$

where $P = \sum_n p_n$ and $Q = \sum_n q_n$. Since all the $\Delta\alpha_n$'s are equal and all the $\Delta\beta_n$'s are equal, we have $\Delta\alpha = \frac{1}{5}[P + (1/\tau)Q]$ and $\Delta\beta = \frac{1}{5}[-Q + (1/\tau)P]$.

To satisfy the first equation in Eqs. (19) it must be possible to find a vector $\mathbf{u}$ and integers p_n and q_n such that

$$\Delta\alpha_n = \mathbf{u}\cdot\mathbf{e}_n + p_n + \frac{1}{\tau}q_n . \tag{D2}$$

We first look for a solution in which $\mathbf{u} = c\mathbf{e}_0$. The zero component of Eq. (D2) requires

$$c = \frac{1}{5}\left[P - 5p_0 + \frac{1}{\tau}(Q - 5q_0)\right] .$$

Using this value of c in the other components of Eq. (44) yields

$$p_n + \frac{q_n}{\tau} = \begin{cases} \left[\left[\frac{5q_0 + 2P - Q}{10} \right] + \frac{1}{\tau} \left[\frac{5p_0 - 5q_0 - P + 3Q}{10} \right] \right], & \text{for } n = 1,4 \\ \\ \left[\left[\frac{-5p_0 - 5q_0 + 3P + Q}{10} \right] + \frac{1}{\tau} \left[\frac{-5p_0 + P + 2Q}{10} \right] \right], & \text{for } n = 2,3 . \end{cases}$$ (D3)

In order to satisfy these equations, each term in parentheses must equal an integer (corresponding to p_n or q_n). For the last term, this implies that $P + 2Q = 5k$ for some integer k. In fact, this condition is sufficient to guarantee that a set of integers p_n and q_n exist which satisfy Eq. (D3). For example, if we choose $p_0 = k$ and $q_0 = Q$, Eq. (D3) implies $p_{1,4} = k$, $p_{2,3} = k - Q$, and $q_{1,4} = q_{2,3} = 0$, all of which are integers. The second equation in Eqs. (19) can be satisfied for the same choice of p_n and q_n with $\mathbf{v} = c' \mathbf{e}_0$ where

$$c' = -(Q - 5q_0) + \frac{1}{\tau}(P - 5p_0) .$$

To see that a different choice for $\mathbf{u}$ would not yield any new possibilities one need only note that the addition to $\mathbf{u}$ of a component perpendicular to $\mathbf{e}_0$ does not alter the quantities $\Delta\alpha_0$, $(\Delta\alpha_1 + \Delta\alpha_4)$, and $(\Delta\alpha_2 + \Delta\alpha_3)$. The conditions on P and Q remain unchanged, although different values of p_0 and q_0 might work.

There are five distinct solutions for (P,Q): $(1,2)$, $(-1,-2)$, $(2,-1)$, $(-2,1)$, and $(0,0)$. All others are equal mod_5 and correspond to umklapping one of these solutions (i.e., a completely equivalent pentagrid). From the expressions,

$$\Delta\alpha \equiv \alpha_n - \alpha_n^* = \frac{1}{5} \left[P + \frac{1}{\tau} Q \right]$$

and

$$\Delta\beta \equiv \beta_n - \beta_n^* = \frac{1}{5} \left[-Q + \frac{1}{\tau} P \right] ,$$

and the expressions for α_n^* and β_n^* given in Eqs. (10) and (11), we can find the associated values of $\{\alpha_n, \beta_n\}$. The solution $(0,0)$ turns out to give $\beta_n = 0$, which is in the ideal and therefore must be examined separately. The correct treatment of this case reveals that it does not deflate to a locally isomorphic tiling. The other four pairs give four patterns that transform into one another under repeated deflation. The values obtained from $(1,2)$ are

$$\alpha = \frac{6\tau - 1}{2(\tau + 2)} \quad \text{and} \quad \beta = \frac{-2}{\tau + 2} .$$

To complete the logic of the argument we note that we have justified our initial assumption (that a symmetric solution for $\{\alpha_n, \beta_n\}$ exists) by exhibiting four explicit examples.

Note that we have not considered the possibility of a PLI class tiling in which $\{\alpha_n, \beta_n\}$ is not locally isomorphic to its deflation, but is locally isomorphic to a rotation or an inversion of its deflation.[2] We do not consider this possibility because we already know that the dual, the Penrose tiling, does not have this property.

[1]D. Levine and P. J. Steinhardt, preceding paper, Phys. Rev. B **34**, 596 (1986).

[2]For simplicity of discussion, we will use a slightly more restrictive definition of LI class in this paper compared to paper I. The definition in Sec. IV A groups configurations related by translations, but not rotations or inversions. See Sec. IV A, Appendix A, and Appendix D for the discussion of the generalization of "LI class" to include rotations and inversions.

[3]D. Levine and P. J. Steinhardt, Phys. Rev. Lett. **53**, 2477 (1984).

[4]P. Kramer and R. Neri, Acta Crystallogr. Sect. A **40**, 580 (1984).

[5]P. A. Kalugin, A. Kitaev, and L. Levitov, JETP **41**, 119 (1985).

[6]V. Elser, Acta Crystallogr. Sect. A **42**, 36 (1986).

[7]M. Duneau and A. Katz, Phys. Rev. Lett. **54**, 2688 (1985).

[8]J. E. S. Socolar, P. J. Steinhardt, and D. Levine, Phys. Rev. B **32**, 5547 (1985).

[9]N. de Bruijn, Ned. Akad. Weten. Proc. Ser. A **43**, 27 (1981); **43**, 39 (1981); **43**, 53 (1981).

[10]F. Gahler and J. Rhyner, J. Math. Phys. A **19**, 267 (1986). Note that these authors have discussed only periodic N-grids, whereas, in this paper, duals of quasiperiodic N-grids, as discussed in Ref. 7, play a crucial role.

[11]R. Penrose, Bull. Inst. Math. Appl. **10**, 266 (1974).

[12]M. Gardner, Sci. Am. **236**, 110 (1977).

[13]S. Kim and J. E. S. Socolar (unpublished).

[14]D. S. Shechtman, I. Blech, D. Gratias, and J. W. Cahn, Phys. Rev. Lett. **53**, 1951 (1984).

[15]B. Grunbaum and G. C. Shepard, *Tilings and Patterns* (Freeman, San Francisco, in press).

[16]N. W. Ashcroft and N. D. Mermin, *Solid State Physics* (Holt, Rinehart and Winston, New York, 1976).

[17]V. Elser (private communication) (in response to Ref. 8).

[18]We note that there are some restrictions on the relative orientations of the $\mathbf{e}_i$ which are necessary to ensure that the tiles do not overlap. These are difficult to express for a general N-grid. They are automatically satisfied for linear and planar N-grids, however, if the $\mathbf{e}_i$'s are taken to be along the grid directions.

[19]Sequences where $0 < \sigma < 1$ can be reexpressed in the form of Eq. (4) for appropriate choices of $\sigma' > 1$, $\rho' > 0$, and an overall rescaling.

[20]C. Radin (unpublished).

[21]G. J. Janusz, *Algebraic Number Fields* (Academic, New York,

1973).

[22]K. B. Stolarsky, Can. Math. Bull. 19, 473 (1976).

[23]E. Bombieri (unpublished).

[24]P. Pleasants, Banach Number Theory Center Publications (unpublished).

[25]R. K. P. Zia and W. J. Dallas, J. Phys. A 18, L341 (1985).

[26]V. Elser, Phys. Rev. Lett. 54, 1730 (1985).

[27]P. Kramer, Z. Naturforsch. Teil A 40A, 775 (1985).

[28]D. Levine, T. C. Lubensky, S. Ostlund, S. Ramaswamy, P. J. Steinhardt, and J. Toner, Phys. Rev. Lett. 54, 1520 (1985).

[29]T. Lubensky, J. E. S. Socolar, and P. J. Steinhardt, Penn preprint (unpublished).
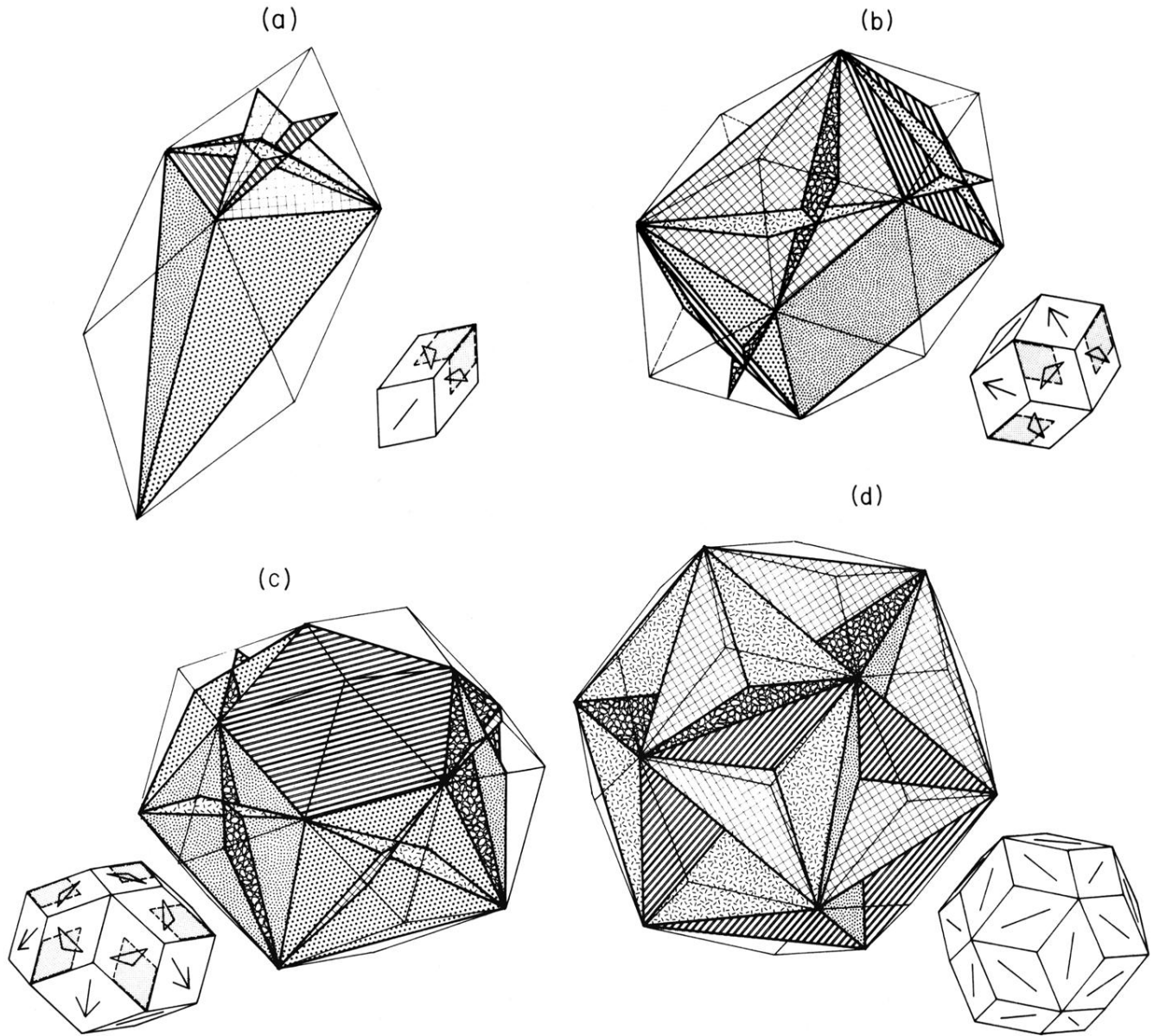
[30]M. Jaric (unpublished).

FIG. 10. Ammann plane decoration of the unit cells of the PLI class packing. A precise specification of the locations of these planes is given in Table II. Parallel planes are shaded the same way. The zonohedra and Ammann planes are shown exactly as they would appear to the eye if the faces of the zonohedra were transparent and the Ammann planes were opaque. In (b), dashed lines indicate edges of the dodecahedron that are seen through transparent faces. A smaller version of each cell is also shown with matching rules and shadings that facilitate comparison with Figs. 11 and 13. (a) The rhombohedron. Its decoration has trigonal symmetry about the long diagonal of the rhombohedron. (b) The dodecahedron. This decoration has two planes of reflection symmetry. One of these reflection planes is nearly perpendicular to the page and contains the long diagonal of the "front" face of the dodecahedron. The other is parallel to the front face and contains the long diagonal of the "top" face (the long edge of the Ammann plane shaded with a square grid). Note that the dodecahedron itself has a third mirror plane, but this symmetry is not respected by the Ammann plane decoration. (c) The icosahedron. This decoration has pentagonal symmetry about the axis of the icosahedron. On the side which is hidden from view is another plane (parallel to the one shaded with double lines) which is intersected by planes forming a star exactly like those found on each plane decorating the triacontahedron in (d). (d) The triacontahedron. The planes of this decoration join to form a perfect great icosahedron.
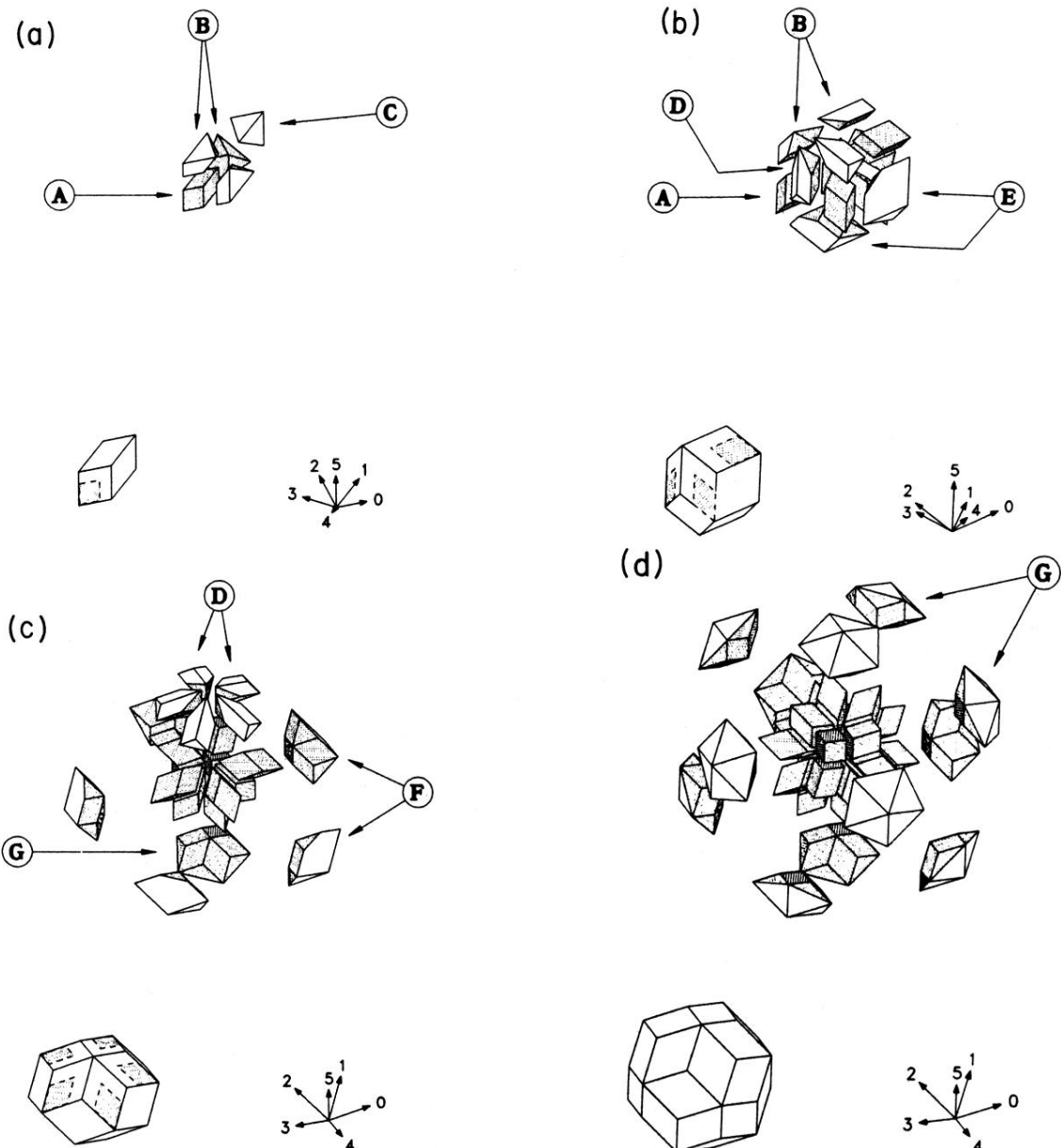
FIG. 11. Deflation decoration of the unit cells of the PLI class packing. Each cell is divided into pieces (labeled A–G) which are shown in exploded views. The faces of the pieces which become faces of the deflated cells are shaded. The unshaded faces adjoin other pieces and lie in the interior of the deflated cells. We have attempted to label enough pieces so that all of them can be identified without cluttering the picture with too many arrows. The precise locations of the vertices of the decoration are given in Table I. The star of vectors in each figure indicates the orientation of each cell as it is described in the table. (a) The rhombohedron deflates to one A, three B's, and one C. (b) The dodecahedron deflates to four A's, two B's, four D's, and two E's. (c) The icosahedron deflates to ten A's, five D's, five F's, and one G. (d) The triacontahedron deflates to twenty A's and twelve G's.
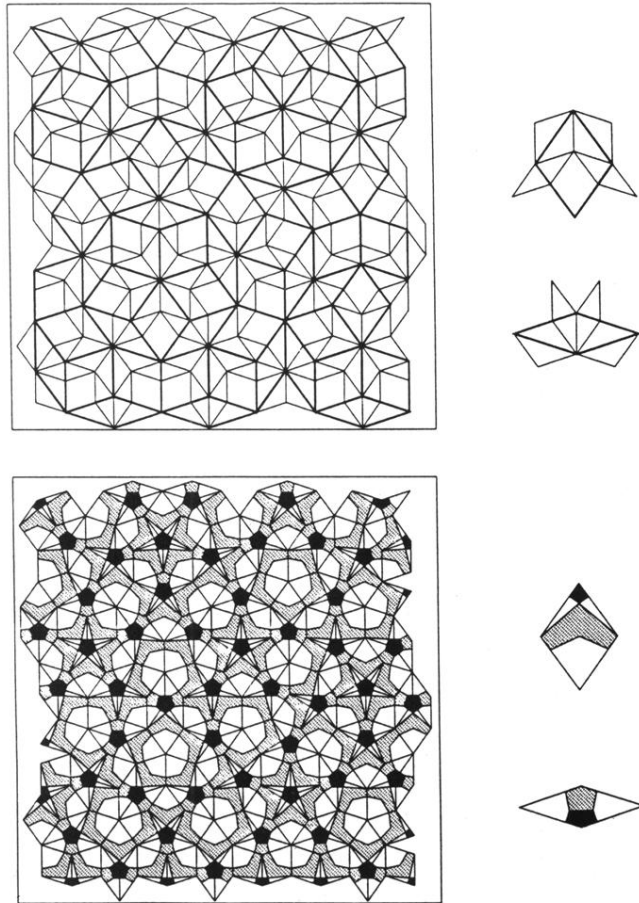
FIG. 4. Two simple decorations of a portion of a Penrose tiling. Top: The deflation decoration. The original tiling (heavy lines) has been decorated as shown at right to form another Penrose tiling (lighter lines). Bottom: A decoration that can be used to enforce the matching rules. According to the matching rules, a pair of tiles can join along an edge only if the strip decorations match across the interface.